DOKUZ EYLÜL UNIVERSITY
GRADUATE SCHOOL OF NATURAL AND APPLIED SCIENCES

PRODUCTION OF SUPERALLOYS VIA SELF PROPAGATING HIGH TEMPERATURE SYNTHESIS AND COATING APPLICATIONS ON STEEL SUBSTRATES

by
Nurdan ARI

October,2023
İZMİR

PRODUCTION OF SUPERALLOYS VIA SELF PROPAGATING HIGH TEMPERATURE SYNTHESIS AND COATING APPLICATIONS ON STEEL SUBSTRATES

A Thesis Submitted to the
Graduate School of Natural and Applied Sciences of Dokuz Eylül University
In Partial Fulfillment of the Requireents for Master of Science in
Department of Metallurgical and Materials Engineering

by
Nurdan ARI

October,2023
İZMİR

M.Sc THESIS EXAMINATION RESULT FORM

We have read the thesis entitled **"PRODUCTION OF SUPERALLOYS VIA SELF PROPAGATING HIGH TEMPERATURE SYNTHESIS AND COATING APPLICATIONS ON STEEL SUBSTRATES"** completed by **NURDAN ARI** under supervision of **ASSOC. PROF.DR. ESRA DOKUMACI ALKAN** and we certify that in our opinion it is fully adequate, in scope and in quality, as a thesis for the degree of Master of Science.

Assoc.Prof.Dr. Esra DOKUMACI ALKAN

Supervisor

Assoc.Prof.Dr. Işıl BİRLİK

Jury Member

Asst.Prof.Dr. Emre ÇİNKILIÇ

Jury Member

Prof. Dr. Okan FISTIKOĞLU

Director

Graduate School of Natural and Applied Sciences

ACKNOWLEDGMENT

First and foremost, I would like to express my sincere appreciation to my advisor, Assoc. Prof. Esra DOKUMACI ALKAN, for her unwavering support throughout my master's program and research. She has consistently demonstrated patience, motivation, enthusiasm, and a wealth of knowledge, all of which have been invaluable to my success.

I would like to express my sincere gratitude to my esteemed Asst.Prof. Dr. Murat ALKAN, for generously sharing his valuable knowledge with me throughout this project. I am truly thankful for his contributions, and I will never forget the significance of every word he used during this experience.

I would like to thank my gratitude to Research Assistants Ramazan DALMIŞ, Özgür Yasin KESKİN and Kadir TEKİN for their invaluable support and contributions throughout my studies.

Once again, I'd like to express my gratitude to Repamet Ltd Şti for their valuable contribution to the analysis.

I would like to express my heartfelt gratitude to my dear mother, Sevim ARI, and my dear father, Tevfik ARI. They have been my greatest source of luck in this life, and have never ceased to support me.

I would like to owe my special thanks to my dear friend Ahmet KAVALAR. Thank you for always being there for me, I truly appreciate your unwavering support.

Nurdan ARI

PRODUCTION OF SUPERALLOYS VIA SELF PROPAGATING HIGH TEMPERATURE SYNTHESIS AND COATING APPLICATIONS ON STEEL SUBSTRATES

ABSTRACT

This study aims to produce a coating layer of Inconel 718 superalloys on a steel substrate using the self-propagating high-temperature synthesis (SHS) method. This method is known for being a fast and low-energy process. In order to obtain the desired alloy composition, a mixture of metal oxide powders, including NiO, Cr_2O_3, Nb_2O_5, MoO_3, TiO_2, Co_3O_4, and Fe_2O_3, as well as reducing Al metal powder, were utilized as raw materials. The exothermic reactions were realized by initiation, and the obtained molten alloys were simultaneously poured on the substrates to form the coating layers. The substrates were made of AISI 1050 alloys having 20 and 40-mm diameters. Furthermore, this study utilized three distinct experimental setups for SHS reactions. Two assemblies were constructed to remain stationary, while the third was rotated at various speeds of 200, 350, and 500 rpm.

The microstructure and mechanical properties of the products were investigated through extensive characterization studies using scanning electron microscopy (SEM), X-ray diffraction (XRD), X-ray fluorescence (XRF), and micro-hardness (micro-Vickers) testing. As a result of the experimental studies, the SHS method is an effective process for coating with solid bonding properties at the interface. It has been observed that the hardness value, which measures the resistance of a material to deformation, increases from the steel substrate to the superalloy coating. Upon closer examination of the interface between the two materials, it is evident that the surface properties of the low alloy steel material have been improved.

Keywords: Inconel 718, Self-propagating High-temperature Synthesis, Coating

KENDİLİĞİNDEN İLERLEYEN YÜKSEK SICAKLIK SENTEZİ İLE SÜPERALAŞIMLARIN ÜRETİLMESİ VE ÇELİK ALTLIKLAR ÜZERİNE KAPLAMA UYGULAMALARI

ÖZ

Bu çalışmanın amacı, hızlı ve düşük enerji gereksinimli, yüksek verimli bir üretim yöntemi olan kendiliğinden ilerleyen yüksek sıcaklık sentezi (SHS) yöntemini kullanarak Inconel 718 süper alaşımını üretip eş zamanlı olarak çelik bir alt tabaka üzerine kaplama yapmaktır. İstenilen alaşım bileşimini elde etmek için NiO, Cr_2O_3, Nb_2O_5, MoO_3, TiO_2, Co_3O_4 ve Fe_2O_3 içeren metal oksit tozları karışımı ile indirgen Al metal tozu hammadde olarak kullanılmıştır. Çelik altlıklar, 20 ve 40 mm çapa sahip AISI 1050 alaşımından seçilmiştir. Ek olarak, bu çalışmada SHS reaksiyonları için üç farklı deney düzeneği kullanılmıştır. Düzeneklerden ikisi sabit şekilde tasarlanmış, üçüncüsü ise 200, 350 ve 500 Rpm gibi çeşitli hızlarda döndürülmüştür.

Taramalı elektron mikroskobu (SEM), X-ışını kırınımı (XRD), X-ışını floresansı (XRF) ve mikro-sertlik (mikro-vickers) testleri kullanılarak ürünlerin mikroyapısı ve mekanik özellikleri kapsamlı karakterizasyon çalışmaları ile incelenmiştir. Sonuçlar incelendiğinde, bir malzemenin deformasyona karşı direncini ölçen sertlik değerinin çelik alt tabakadan süper alaşım kaplamaya doğru arttığı gözlemlenmiş ve böylece düşük alaşımlı çelik malzemenin yüzey özellikleri iyileştirilmiştir. SHS reaksiyonu ile çelik alt tabaka ile süper alaşım kaplama arasında güçlü bir arayüzey bağı elde edilmiştir.

Anahtar kelimeler: Inconel 718, Kaplama, Kendiliğinden ilerleyen yüksek sıcaklık sentezi

CONTENTS

Page

LIST OF FIGURES

Page

LIST OF TABLES

Page

LIST OF SYMBOLS

°C	: Celcius
γ′	: Gamma Prime
γ′′	: Gamma Double Prime
η	: Eta
δ	: Delta
MPa	: Megapascal
T_m	: Melting Temperature
T_{ad}	: Adiabatic Temperature
k	: Thermal Conductivity
Cp	: Heat Capacity
ρ	: Density
Q	: Heat of the Reaction
α	: Degree of Advancement of the Reaction
T	: Temperature
t	: Time
x	: Axis of Wave Propagation

ABBREVIATIONS

SHS	: Self Propagating High Temperature Synthesis
BCC	: Body Centered Cubic
FCC	: Face Centered Cubic
SEM	: Scanning Electron Microscope
APB	: Antiphase Domain Boundary
P/M	: Powder Metallurgy
HIP	: Hot Isostatic Pressing
ODS	: Oxide Dispersion Strengthened
FGM	: Functional Graded Materials
XRF	: X-Ray Fluorescence
EDS	: Energy Dispersive Spectrometer

CHAPTER ONE
INTRODUCTION

At the start of World War II, airplanes were going further and faster than ever before. Scientists had to manufacture new alloys that worked in unexpectedly high temperatures to ensure their metal parts could handle the increased velocity and altitude. In order to withstand oxidation, these alloys must contain chromium, aluminum, or both. Over time, numerous researchers have made concerted efforts to develop these alloys. Many trial-and-error experiments have been conducted to reach this point. Despite the challenges, significant progress has been made in creating exceptional alloys. These studies discovered superalloys (Kracke & Allvac, 2010).

Superalloys are commonly utilized in aircraft turbine engines due to their remarkable heat-resistant properties. They exhibit high levels of strength, an extended fatigue life, superior fracture toughness, creep resistance, stress-rupture resistance, and a capacity to resist corrosion and oxidation at elevated temperatures. These materials can function at temperatures up to 950-1300 °C for extended periods, rendering them well-suited for contemporary jet engines (Mouritz, 2012).

Self-propagating high-temperature synthesis (SHS) is a process that ignites starting reagents with an external effect to create an extremely exothermic reaction that propagates throughout the reaction mixture in the form of a wave. It is also known as combustion synthesis, gasless combustion, or self-propagating exothermic reactions. It has several advantages over other methods, such as producing unique materials that are difficult to obtain otherwise. This method is simple, inexpensive, and has low energy requirements, making it promising for large-scale production of advanced materials. It is used in many fields, including materials science, metallurgy, and nanotechnology, to produce ceramics, metals, and composites with complex phases and high purity (Subrahmanyam, 1992).

CHAPTER TWO
SUPERALLOYS

Superalloys have a long history dating back to 1907. However, the term "superalloy" was not coined until the mid-1940s when cobalt-based alloys like Vitallium and nickel-based Waspaloy were referred to as such. Over the past five decades, significant advancements have been made in alloy development, hot working, heat treating, and process development, enabling the end-use technologies known today (Kracke & Allvac,2010).

Superalloys are renowned for their impressive combination of mechanical strength and surface stability. Superalloys possess several highly desirable properties, such as strength, creep resistance, fracture toughness, fatigue life, and stress-rupture resistance at elevated temperatures. Moreover, they display remarkable resistance to corrosion and oxidation at high temperatures, which is a significant advantage over many other metallic materials that can rapidly deteriorate under such conditions (Mouritz, 2012).

Combining base metals and refractory-metal additives determines the physical properties of superalloys. The presence of these elements leads to lower electrical conductivity, specific heat, thermal conductivity, and thermal expansion compared to other materials. It is worth noting that superalloys come in different types with varying densities. For instance, iron-based superalloys have a density of 7.9 to 8.3 g/cm^3, while cobalt-based superalloys have a density of 8.3 to 9.4 g/cm^3. On the other hand, Nickel-based superalloys have a density of 7.8 to 8.9 g/cm^3. Nevertheless, even though superalloys vary in density, they all possess exceptional properties that make them well-suited for high-temperature applications (Donachie, 2002).

These alloys have found a wide range of applications in high-temperature environments. For instance, they are used as front panels for thermal protection systems, especially in sheet form. These alloys are also commonly found in space components, blades, and vanes in turbine engines, as well as essential components of rocket engines (Rao,2018).

Additionally, they are used in submarines, heat exchangers, chemical processing vessels, and nuclear reactors. The versatility of these alloys is genuinely remarkable, and they continue to be used in new and innovative ways (Rao,2018).

2.1 Microstructure of Superalloys

Superalloys comprise an austenitic face-centered cubic (fcc) matrix phase and a γ variety of secondary phases that control their properties. The secondary phases that are most valuable in this regard are the fcc carbides MC, $M_{23}C_6$, M_6C, and M_7C_3, which are present in virtually all types of superalloys. Other critical phases include; gamma prime (γ′ - an fcc ordered phase $Ni_3(Al,Ti)$), gamma double prime(γ″ - a body-centered cubic ordered phase Ni_3Nb), eta (η - a hexagonal ordered phase Ni_3Ti), and delta (δ - an orthorhombic intermetallic compound Ni_3Nb), which are found in nickel- and iron-nickel-base superalloys. The γ′, γ″, and η phases are also referred to as geometrically close-packed phases. The SEM image of the superalloy is presented in Figure 2.1. Superalloys possess unique properties due not only to their grain size and morphology but also to the production and manipulation of their various phases, including occasional cold work (Donachie, 2002).

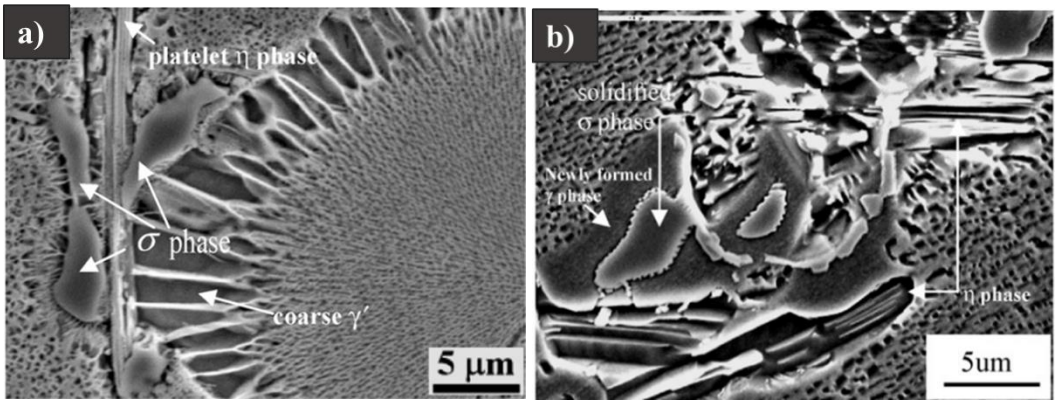

Figure 2.1 SEM micrograph a) In the vicinity of the interdendritic region b) The formation of the σ phase, specifically in a nodular form, after undergoing a solution treatment process (Long, 2009)

Carbides are vital to superalloys, especially those not in single-crystal form. They are significant in the grain boundaries of cast alloys to attain the desired strength and ductility properties. Although wrought alloys have traditionally had lower levels of carbides than cast alloys, some carbide is still necessary for achieving the best strength characteristics. As superalloys have become cleaner, the amount of carbide in wrought alloys has decreased. Carbides, especially large ones, can be a limiting factor in modern wrought superalloy applications due to their potential impact on fracture mechanics. Specific carbides can enhance the strength of the cobalt-base superalloy matrix, while others are essential for controlling grain size in specific wrought alloys. Carbides can vary in their susceptibility to heat treatment, and their composition can depend on the alloy and processing used. SEM microstructure images of various carbides are shown in Figure 2.2 (Donachie, 2002).

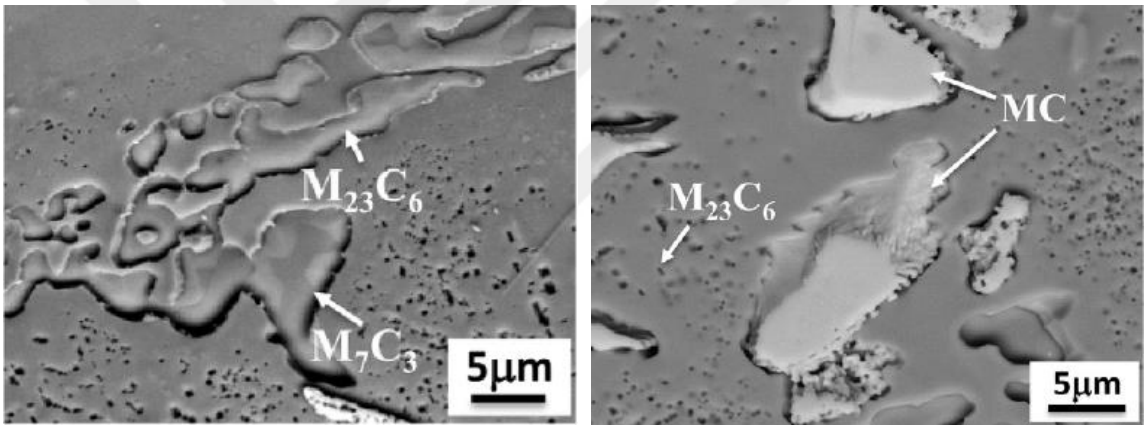

Figure 2.2 SEM micrographs of some carbide precipitates (Gui,2016)

Superalloys derive their strength mainly from solid-solution hardeners and precipitated phases. The primary strengthening precipitate phases are gamma prime and gamma double prime, present in iron-nickel- and nickel-base superalloys. Carbides can provide limited direct or indirect strengthening and are found in all three superalloy groups. Delta and eta phases, along with gamma prime, are useful in controlling the structure of wrought iron-nickel- and nickel-base superalloys during processing. The extent to which they improve strength is determined by the particular alloy and its processing. Table 2.1 demonstrates how alloying elements function in superalloys (Donachie, 2002).

Table 2.1 The function of alloying elements in superalloys (Donachie, 2002)

Effect	Iron Base	Cobalt Base	Nickel Base
Solid solution strengtheners	Cr, Mo	Nb, Cr, Mo, Ni, W, Ta	Co, Cr, Fe, Mo, W
fcc matrix stabilizers	C, W, Ni	Ni	….
Carbide form:			
MC	Ti	Ti	W, Ta, Ti, Mo, Nb, Hf
M_7C_3	….	Cr	Cr
$M_{23}C_6$	Cr	Cr	Cr, Mo, W
M_6C	Mo	Mo, W	Mo, W, Nb
Carbonitrides : M(CN)	C, N	C, N	C, N
Forms γ′ Ni_3(Al, Ti)	Al, Ni, Ti	….	Al, Ti
Hardening precipitates and/or intermetallics	Al, Ti, Nb	Al, Mo, W, Ta	Al, Ti, Nb

To improve mechanical or chemical properties, elements such as boron, zirconium, and hafnium are minorly added alongside the main elements that create solid-solution hardening or encourage carbide and γ′ formation. These additional elements are typically absent from most cobalt-based alloys. Certain carbide and γ′ forming elements can also notably affect chemical properties. In iron-nickel- and nickel-based superalloys, borides may form (Donachie, 2002).

2.2 Classification of Superalloys

Superalloys, a type of high-performance material used in extreme environments, can be classified into three major categories. The first category is based on the primary element used in the alloy, such as nickel, cobalt, or iron. The second category is based on the mechanism used to strengthen the alloy, such as solid solution strengthening, precipitation strengthening, or dispersion strengthening. Finally, the third category is based on the production method used to create the alloy, such as casting, forging, or powder metallurgy (Mouritz, 2012).

Each of these categories plays a crucial role in determining the properties and performance of the superalloy, making it a versatile and essential material in various industries, including aerospace, power generation, and chemical processing (Reed & Rae, 2014). The classification of superalloys is shown in Figure 2.3.

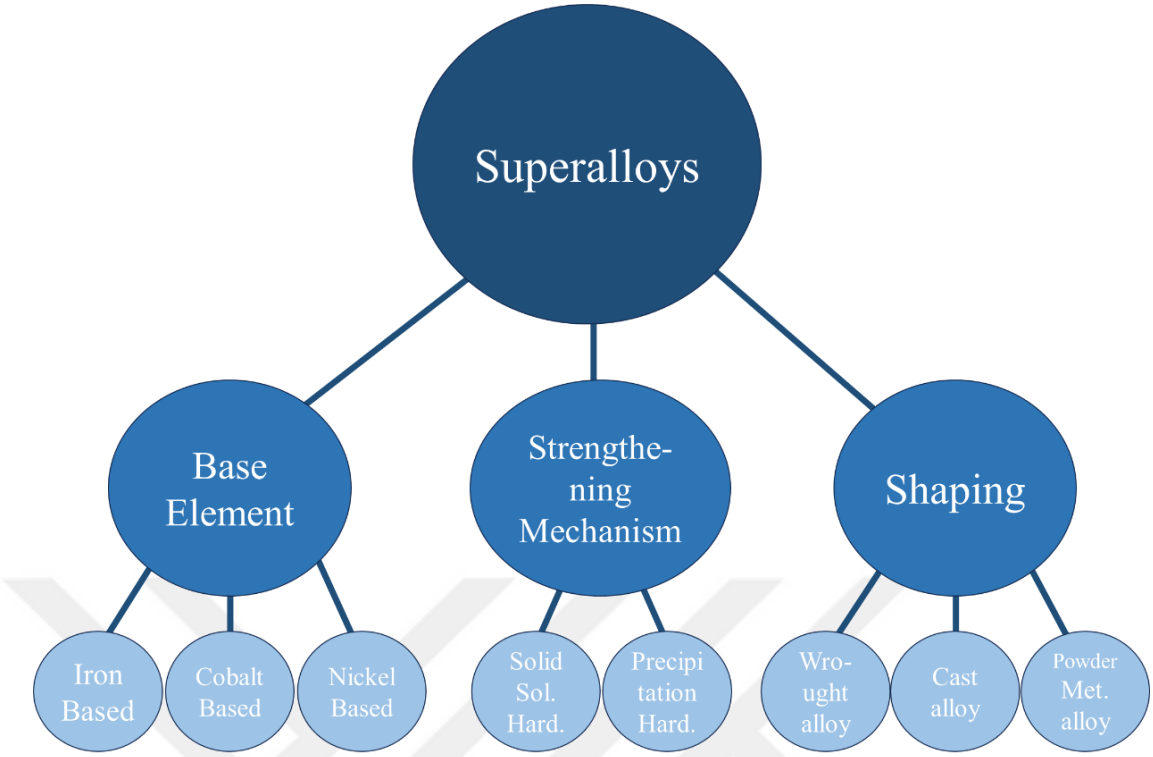

Figure 2.3 Classification of superalloys (Reed & Rae, 2014)

2.2.1 Classification by the Base Element

2.2.1.1 Iron Based Superalloys

Iron-nickel superalloys are widely used in gas turbine engines for their excellent structural properties and low thermal expansion at high temperatures. They are ideal for engine components requiring tight clearances between rotating parts, as they expand less than nickel or cobalt superalloys at high temperatures. In addition to their superior performance, iron-nickel alloys are more cost-effective than other superalloys, making them a popular choice in the aerospace industry (Mouritz, 2012).

Iron-nickel alloys can contain varying amounts of iron and nickel, with the most commonly used alloys containing between 15-60% iron and 25-45% nickel. The hardness of these alloys is achieved through a combination of solid solution strengthening and precipitation strengthening. Alloy elements like aluminum, niobium, and carbon are utilized to encourage the creation of hard intermetallic precipitates or carbides that stay stable at elevated temperatures (Mouritz, 2012).

These precipitates enhance the performance of iron-nickel alloys, imparting excellent resistance to creep and stress rupture at high temperatures. This property makes them a suitable choice for use in jet engines. Table 2.2 provides examples of iron-based superalloys, their corresponding ultimate tensile strength, yield strength, and elongation values (Donachie, 2002).

Table 2.2 Some examples of iron-based superalloys along with their ultimate tensile strength, yield strength, and elongation values (Donachie, 2002)

	Ultimate Tensile Strenght (Mpa) at:			**Yield Tensile Strenght (Mpa) at 0,2% offset at**			**Tensile Elongation % at**		
Alloy	**21 °C**	**540 °C**	**760 °C**	**21 °C**	**540 °C**	**760 °C**	**21 °C**	**540 °C**	**760 °C**
Haynes 556	815	645	470	410	240	220	48	54	49
Incoloy 801	785	660	325	385	310	290	30	28	55
N155	815	650	428	400	340	250	40	33	32
V57	1170	1000	620	830	760	485	26	19	34

The presence of various types of carbides and intermetallic precipitates, such as γ′ and γ″ characterizes the microstructure of iron-nickel alloys. These precipitates are similar to those found in nickel-based superalloys and play a critical role in the mechanical properties of the material. Chromium also forms an oxide surface layer that protects the metal from corrosive gases and oxidation (Mouritz, 2012).

In addition to their use in blades, discs, and casings, iron-nickel superalloys have a wide range of potential applications in the aerospace industry (Mouritz, 2012).

Ongoing research is focused on developing new alloys with improved mechanical properties and excellent resistance to high-temperature oxidation and corrosion. As the demand for more efficient and reliable gas turbine engines grows, iron-nickel superalloys will likely remain critical in the aerospace industry for years (Mouritz, 2012).

2.2.1.2 Cobalt Based Superalloys

Cobalt-based superalloys are a promising group of materials for the next generation of superalloys. These materials offer several advantages over nickel-based superalloys, such as higher melting temperatures, better oxidation resistance, and superior wear resistance. As a result, cobalt-based superalloys can operate at higher temperatures than nickel-based superalloys, leading to improved turbine efficiency and significant fuel cost savings (Jokisaari,2017).

Although cobalt-based superalloys have been used for decades in static, low-stress service conditions, their poor creep resistance has limited their use in high-stress applications. However, researchers have been working to overcome this limitation in recent years by developing new cobalt-based superalloys with improved creep resistance (Jokisaari,2017).

Table 2.3 provides examples of cobalt-based superalloys, their corresponding ultimate tensile strength, yield strength, and elongation values. Moreover, it is important to note that caution should be exercised when comparing nickel and cobalt alloys due to the significant variations in hot corrosion resistance within each superalloy group (Donachie, 2002).

Table 2.3 Some examples of cobalt based superalloys along with their ultimate tensile strength, yield strength, and elongation values (Donachie, 2002)

	Ultimate Tensile Strenght (Mpa) at:			**Yield Tensile Strenght (Mpa) at 0,2% offset at**			**Tensile Elongation % at**		
Alloy	**21 °C**	**540 °C**	**760 °C**	**21 °C**	**540 °C**	**760 °C**	**21 °C**	**540 °C**	**760 °C**
Haynes 188	960	740	635	485	305	290	56	70	43
MP159	1895	1565	-	1825	1495	-	8	8	-

Cobalt alloys contain about 30–60% cobalt, 10–35% nickel, 20–30% chromium, 5–10% tungsten, and less than 1% carbon. This unique composition provides several benefits (Donachie, 2002).

These materials possess excellent mechanical properties derived from solid solution strengthening and carbide precipitation strengthening. The latter is significant, as it provides additional strength and durability to the material. In addition to their use in turbines, cobalt-based superalloys have also found applications in other high-temperature environments, such as oil and gas, where they are used in drilling and exploration equipment (Gui,2019).

2.2.1.3 Nickel Based Superalloys

Because of their superior mechanical and chemical properties, nickel-based superalloys are widely used in various industries, including marine, aerospace, nuclear reactors, and chemicals. Table 2.4 shows examples of nickel-based superalloys and their respective ultimate tensile strength, yield strength, and elongation values (Donachie, 2002). These alloys are typically composed of at least 50% nickel and more than ten types of alloying elements, including high amounts of chromium (10-20%), aluminum, titanium (up to 8% combined), and cobalt (5-15%), as well as small amounts of molybdenum, tungsten, and carbon (Mouritz, 2012).

The high chromium content of these alloys helps to create a protective surface layer of chromium oxide (Cr_2O_3) that protects the nickel from oxidation and hot corrosion. Additionally, the presence of molybdenum, chromium, cobalt, and tungsten strengthens the nickel by solid solution hardening. Meanwhile, the addition of aluminum, titanium, and carbon help to strengthen the nickel alloys by hard intermetallic precipitates and carbides (Mouritz, 2012).

Table 2.4 Examples of nickel based superalloys, along with their respective ultimate tensile strength, yield strength, and elongation values (Donachie, 2002)

	Ultimate Tensile Strenght (Mpa) at:			**Yield Tensile Strenght (Mpa) at 0,2% offset at**			**Tensile Elongation % at**		
Alloy	**21 °C**	**540 °C**	**760 °C**	**21 °C**	**540 °C**	**760 °C**	**21 °C**	**540 °C**	**760 °C**
Inconel 625	965	910	550	490	415	415	50	50	45
Inconel 718	1435	1275	950	1185	1065	740	21	18	25
Hastelloy S	845	775	575	455	340	310	49	50	70
Nimonic 90	1235	1075	655	810	725	540	33	28	12
Astroloy	1415	1240	1160	1050	965	910	16	16	21

In aerospace, nickel-based superalloys are used to construct turbine blades and other high-temperature components due to their ability to withstand extreme temperatures and stresses. In marine and chemical industries, these alloys are used in pumps, valves, and other critical components that require resistance to corrosion and erosion. In nuclear reactors, these alloys are used in fuel rods due to their ability to withstand the high temperatures and radiation levels found in nuclear reactors (Mouritz, 2012).

Nickel superalloys strengthen from solid solution hardening or a combination of solid solution and precipitation hardening. Superalloys that rely mainly on solid solution strengthening contain strong substitutional strengthening elements such as molybdenum and tungsten. While solid solution-hardened nickel alloys offer good corrosion resistance, their high-temperature properties do not match those of precipitation-hardened alloys. As illustrated in Figure 2.4, nickel-based superalloys can be hardened through the solid solution or precipitation strengthening to increase their creep-rupture strength (Mouritz, 2012).

Nickel superalloys that harden by precipitation strengthening offer excellent high-temperature performance and are commonly utilized in various parts of jet engines, including blades, shafts, rings, discs, and compressor components. Precipitation-hardened nickel alloys are also used in rocket motor engines. The precipitation-hardened nickel alloys include aluminum, titanium, tantalum, or niobium. During heat treatment, these elements react with the nickel to form small, hard intermetallic precipitates dispersed throughout the alloy (Mouritz, 2012).

The most significant precipitate is γ′. These highly thermally stable precipitates provide strength and creep resistance at high temperatures. A high volume fraction of γ′ precipitates is required for high strength, fatigue resistance, and creep properties (typically above 50%). The γ′ precipitates are created via a heat-treatment process that includes solution treatment followed by thermal aging to dissolve the alloying elements into a solid solution (Mouritz, 2012).

Creep is a material property essential to ensuring engine components' long-term reliability. It refers to the permanent distortion and plastic yielding of materials when

subjected to elastic loads, which is particularly important in high-temperature applications (Mouritz, 2012).

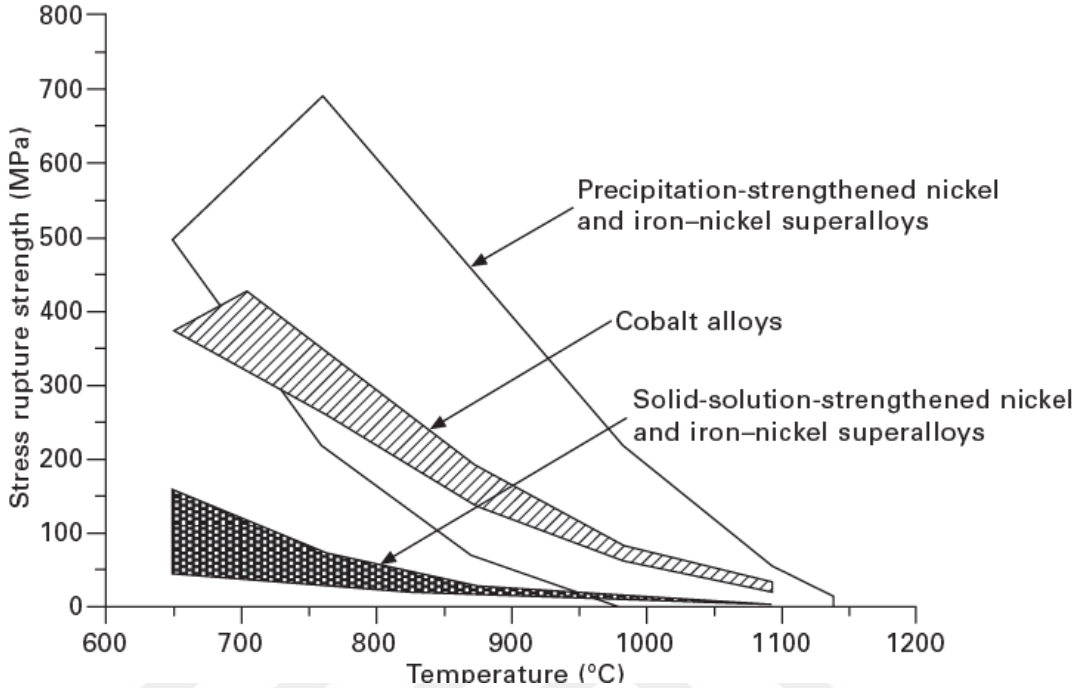

Figure 2.4 The creep-rupture strength of superalloys based on nickel after hardening (Mouritz, 2012)

At temperatures ranging from 30 to 40% of their melting temperature, materials can experience rapid creep. For example, materials such as aluminum and titanium alloys, widely utilized in cooler regions of jet engines, tend to experience quick creep at temperatures above 150 and 350 °C, respectively (Mouritz, 2012).

On the other hand, nickel superalloys are known for their exceptional creep resistance, enabling them to be used at temperatures as high as 850 °C, over 70% of their melting temperature (Tm: 1280 °C). Nickel superalloys are particularly noteworthy for their exceptional creep and stress rupture resistance, which allows engines to operate at higher temperatures and produce greater thrust. Nickel-based alloys demonstrate exceptional stress rupture strength compared to materials utilized in aircraft structures, including titanium, aluminum, and magnesium alloys (Mouritz, 2012).

Among the various types of alloys, the most significant one used in aerospace is Inconel 718. It is renowned for its high strength and resistance to corrosion, making it ideal for use at temperatures around 750 °C. Inconel 718 is a high-performance nickel-chromium alloy due to its superior properties, such as high strength, corrosion resistance, and excellent creep and fatigue resistance (Mouritz, 2012).

However, its alloy-specific thermomechanical properties and low thermal conductivity cause significant difficulties in machining due to its high hardness (Pusavec,2014).

The machining of Inconel 718 is challenging, and existing machinability problems can be eliminated with a machining process called cryolubrication. This process involves using a coolant and lubricant mixture that is applied at very low temperatures, and it has been shown to provide excellent results. Cryolubrication can significantly reduce tool wear and cutting forces and improve surface roughness when machining Inconel 718 (Pusavec,2014).

2.2.2 Classification by the Strength Mechanism

Polycrystalline materials deform through the deformation of individual grains and the movement of those grains within the material. The extent of each mechanism depends on the temperature, composition, and microstructure. At temperatures below $0.6T_M$, most deformation occurs within grains. At temperatures higher than $0.6T_M$, there can be sliding of grain boundaries, which causes the grains to move and rotate relative to each other. The properties of grain boundaries are influenced by the carbides formed in these areas and the characteristics of the grain boundaries themselves (Rao,2018).

2.2.2.1 Solid Solution Hardening

Solid solution hardening is a metallurgical process that involves adding soluble elements like chromium, tungsten, cobalt, molybdenum, rhenium, and ruthenium to increase the strength of a metal's matrix. The process works by distorting the atomic lattice structure, which inhibits dislocation movement due to the fit of the atomic radius (Liu et al., 2020).

It is worth noting that the extent of solid solution hardening varies with the atomic size difference, and it reaches a maximum difference of over 10%. For instance, the difference in atomic diameter from that of nickel varies from +1% for cobalt to +13% for tungsten (Liu et al., 2020).

The creep strength of nickel-based superalloys is significantly influenced by the solid solution strengthening of the γ matrix. To achieve this, rhenium, tungsten, molybdenum, and ruthenium are commonly used, while chromium and cobalt are less effective. These elements are highly effective in strengthening the γ phase, especially at high creep temperatures. The diffusion coefficient in the γ matrix determines their ability to serve as solid solution strengtheners. For instance, rhenium is considered the most effective element for improving the creep properties of nickel-based single-crystal superalloys. This is primarily due to its low diffusion coefficient compared to other alloying elements (Liu et al., 2020).

The significance of solid solution strengthening in the γ matrix cannot be overstated. It is a complex process that involves the interaction of these elements with dislocation movement in the γ matrix. The exact mechanism of this interaction is still not fully understood, even with technological advancements. However, researchers have made significant progress in identifying the essential elements and their role in the solid solution strengthening of the γ matrix (Liu et al., 2020).

2.2.2.2 Precipitation Hardening

Precipitates strengthen an alloy by impeding the deformation process that occurs under load. Specific primary hardening precipitate characteristics that obstruct deformation include:

- The level of difference between the precipitate and matrix should be considered. The ideal scenario is when the matrix and precipitate share the same crystal structure and nearly identical crystal lattice sizes. This creates the potential to pack more precipitate into the gamma phase of the matrix. In iron-nickel base and nickel-base superalloys, mismatches can vary from 0 +/- to around 1% (Donachie, 2002).

-The introduction of preferred positions (ordering) for individual atoms in a material result in a more energy-intensive process for passing deformation elements (dislocations) through a precipitate. This is due to the increased energy required to overcome the energy associated with ordered atom positions, known as the antiphase domain boundary (APB), compared to normal, disordered, or random positions. As the APB energy increases, the force required for deformation also increases (Donachie, 2002).

-The size of precipitates can significantly affect the behavior of crystals. If the size is too small, dislocations may easily pass through the crystal. Conversely, if the size is too large, dislocations may bow, and the strength of the crystal may be lower than desired. The optimal size of precipitates is dependent on the specific property being measured (Donachie, 2002).

2.2.3 Classification by the Shaping

2.2.3.1 Cast Superalloy

Investment casting molds can be created using the solid investment or ceramic shell process, although the latter is more commonly used in engineering applications. This process involves constructing a shell from refractory aggregate and a silicate binder, casting molten superalloy into the shell, and creating castings with finely detailed surface finishes and accurate dimensions. Patterns for investment casting are fashioned from wax or plastic, with wax patterns being more commonly used (Donachie, 2002).

Hollow castings that feature intricate internal details are crafted by producing a ceramic core, placing it into a wax injection die, and enveloping it with wax to create a wax pattern that takes on the desired form of the final part. The fundamental steps in this process are depicted in Figure 2.5 (Donachie, 2002).

The investment casting process involves attaching wax patterns to a tree, coating the tree in ceramic through multiple dips, burning out the wax, and firing the ceramic to create a mold tree with individual article molds attached for casting with molten metal (Donachie, 2002).

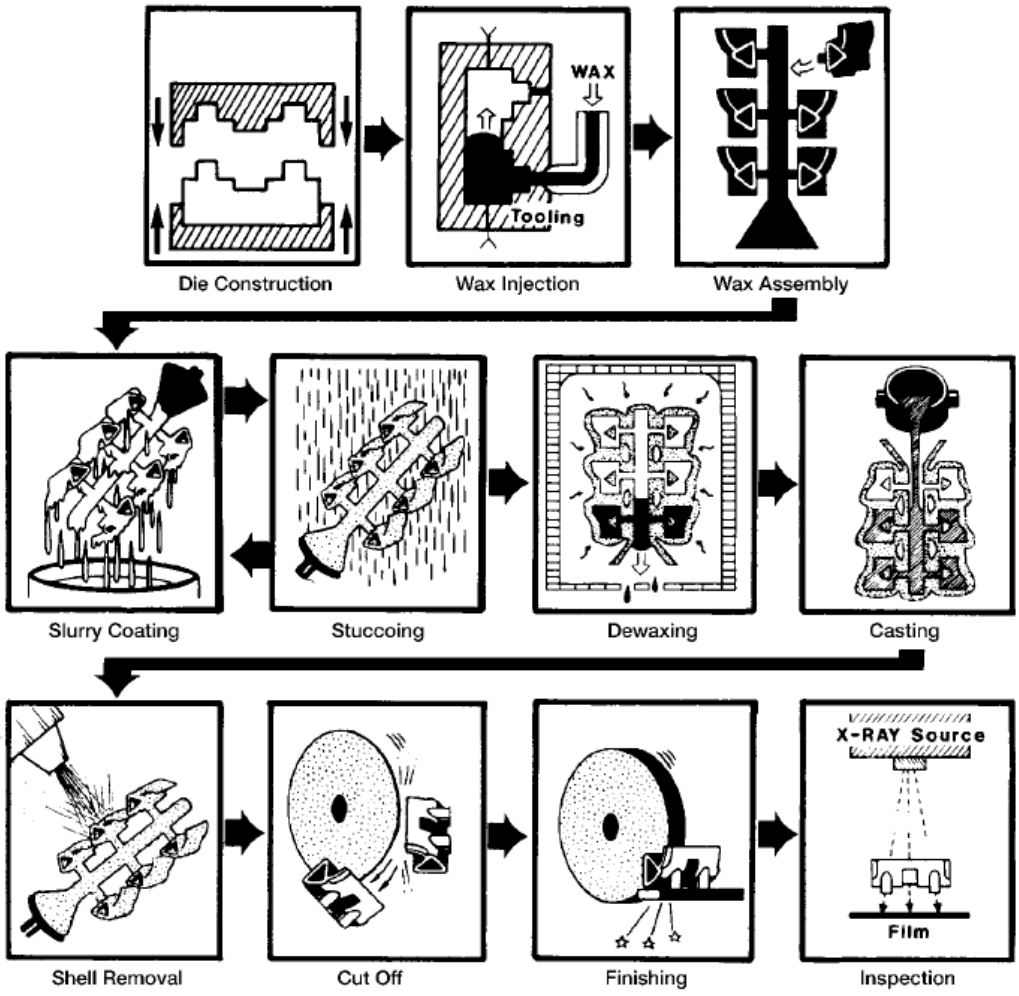

Figure 2.5 Schematic representation of the investment casting process (Donachie, 2002)

To create the desired product, the metals are melted and poured into a mold, which is then solidified under specific conditions depending on the size and type of product being produced. The quality of the final part hinges on the mold used.The ceramic material of the mold must withstand the molten metal without being significantly attacked (i.e., no mold-metal reaction) (Donachie, 2002).

However, the ceramic should be able to dissolve in an appropriate base, allowing for easy cleaning of passages or external surfaces without any deformation of the metal due to mechanical processing (Donachie, 2002).

The usage of investment castings in aircraft gas turbines, particularly for turbine airfoils, has revolutionized the industry by providing a superior alternative to forged airfoils. Castings are more robust at elevated temperatures due to their larger grain size, and the development of air-cooled cast airfoil designs has further increased durability and stability in high-temperature applications. The progress in alloy and investment process development has resulted in intricate internal passages in turbine airfoils that have significantly improved their functionality (Donachie, 2002).

2.2.3.2 Wrought Superalloy

Wrought superalloys are materials widely used in several industries, including aerospace, automotive, and oil and gas. These alloys are typically produced by remelting vacuum induction melting ingots, which are then formed into a secondary ingot or powder. Wrought alloys require a secondary melting process to ensure the high-temperature structural properties of Ni-based superalloys are consistent. Because of the microstructure, chemical composition, and impurities can significantly affect their properties. For instance, when the microstructure is not homogeneous, it can lead to a wide range of mechanical properties of the alloy. Additionally, the presence of impurities and variations in chemical composition can also adversely affect the performance of the alloy, leading to reduced durability and increased wear and tear (Donachie, 2002).

When ingots are large, there is a risk of macro segregation or the formation of large shrinkage cavities during solidification when using vacuum induction melting. Solidification defects are typically the result of solute segregation that occurs during dendritic solidification under low thermal gradients on a large scale. Because the solidifying mass of vacuum induction melting ingots has a low intrinsic thermal conductivity, heat transfer during solidification is limited. This means that large ingots are particularly prone to forming these features (Donachie, 2002).

Therefore, other secondary melting processes such as electro-slag remelting, vacuum arc remelting, and electron beam cold hearth refining are utilized in order to prevent these issues (Akca,2015).

Additionally, these secondary melting processes also offer benefits such as improved homogeneity of the microstructure, reduced impurities, and increased control over the chemical composition of the final product. For example, vacuum arc remelting ensures better mixing of the molten metal, leading to a more uniform microstructure. Electro-slag remelting, on the other hand, reduces impurities in the alloy by using a slag layer to filter out unwanted elements. Finally, electron beam cold hearth refining allows for precise control over the chemical composition of the alloy by adding or removing specific elements as required (Akca,2015).

The main methods for plastic forming superalloys are extrusion, extrusion-forging, and extrusion-rolling. The feasibility of these processes depends on the alloy content and ingot structure. After the extrusion or rolling processes, a homogenization heat treatment is performed. The extrusion also creates the appropriate grain size for isothermal superplastic forging applications. It is important to note that not all types of alloys can be formed economically using all techniques. For example, Ni and Fe-Ni-based superalloys are commonly forged using a hammer or press. The forging process is applied under a constantly falling temperature as the workpiece is taken from the preheating furnace and transferred to the mold at a lower temperature. Patterns and isothermal forging have been applied in recent years by maintaining the same temperature by heating or insulating the part. By using extrusion and rolling, the final product with homogeneous grain size is obtained by annealing in general (Çay,2005).

However, some superalloys that do not require high-temperature applications can be formed by cold working. Forging processes can be applied according to one of two different approaches. The first approach focuses on cost, providing the desired mechanical properties through annealing and producing the most suitable geometric shapes with the cheapest means. The second approach focuses on the microstructure of the material, which is achieved through thermomechanical processes (Çay,2005).

2.2.3.3 Powder Metallurgy

Powder metallurgy (P/M) techniques are widely used in producing nickel-base superalloys. These techniques are primarily utilized to create high-strength gas turbine disk alloy compositions, like IN-100 or Rene 95, which are difficult or impractical to forge using conventional methods. They are also used to a limited extent for oxide-dispersion-strengthened (ODS) alloys in airfoils. The powder metallurgy process offers an advantage over conventional ingot metallurgy processes by creating homogeneous, fine-grained billets or preforms from highly alloyed nickel-base alloys. This results in closer control of microstructure within a part than is possible with cast and ingot metallurgy wrought products (Donachie, 2002).

Near-net shape processes have lowered costs by minimizing the critical raw materials required and reducing the need for additional machining. Powder metallurgy processing provides greater control over a part's microstructure compared to cast and ingot metallurgy wrought products. Several methods can create a near-net shape part with reduced raw material input for producing a specific gas turbine component, such as a compressor disk. These methods include conventional ingot metallurgy and hot isostatic pressing (HIP) with or without forging. Actual savings on raw materials will vary based on the P/M route selected and the component's complexity. The utilization of direct HIP, or hot isostatic pressing, has been demonstrated to reduce the amount of material input needed from 210 to 40 pounds or 95 to 18 kilograms. This, in turn, not only enhances process efficiency but also mitigates waste and reduces costs. Figure 2.6 shows how much raw material can be saved when producing a gas turbine part (compressor disk) using conventional ingot metallurgy, hot isostatic pressing (HIP) plus forging, and direct HIP to create a near-net shape part (Donachie, 2002).

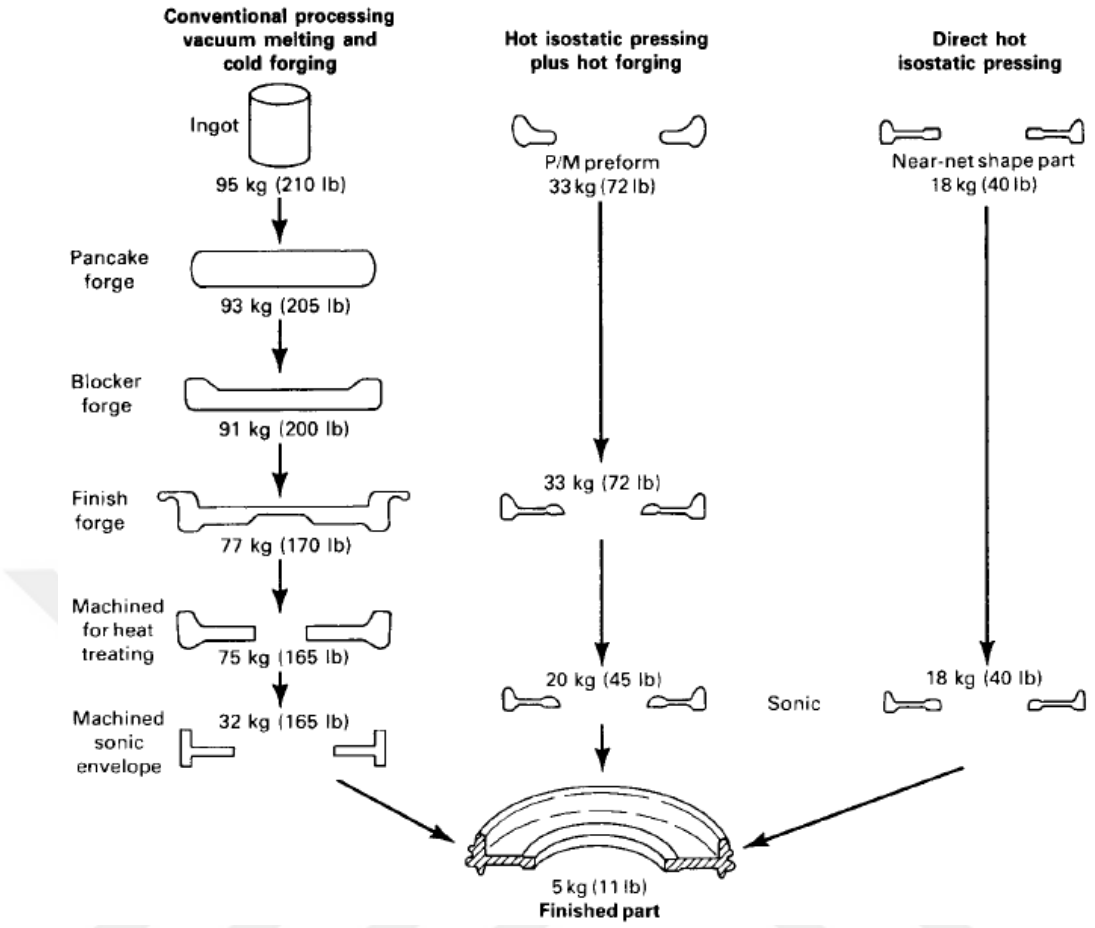

Figure 2.6 Possible sequences for processing a gas turbine compressor disk, which demonstrate how P/M superalloy technology can help reduce the weight of the input material (Donachie, 2002)

Powder metallurgy can produce a variety of alloys. Some examples include Rene 95, Udimet 720, IN-706, and IN-718 for chemical applications, GE T700 and GE F110 for engine systems, and Stellite 31, Astroloy, and Merl 76 for aviation (Donachie, 2002).

2.3 Heat Treatment of Superalloys

Superalloys require heat treatment to prepare them for further processing and chemical treatments. Heat treatment can achieve many goals, such as reducing stress, redistributing alloy elements, promoting grain growth and new grain formation, dissolving or producing new phases, and changing surface chemistry with foreign atoms. Heat treatment is essential in creating optimal properties for many superalloy applications (Donachie, 2002).

Superalloys often undergo several heat treatment steps during processing to develop properties or complete a chemical treatment. There are several types of heat treatments, but some of the most frequently used are stress relief, solution annealing, in-process annealing, full annealing, coating diffusion, and precipitation (age) hardening. Each of these treatments is designed to achieve specific results, depending on the type of metal or alloy being treated and the desired properties (Donachie, 2002).

Many important processes are involved in manufacturing but are often ignored or undervalued. For example, applying a thermal shock test to an airfoil is necessary to ensure its durability. Similarly, welding or brazing an alloy requires high precision and expertise, as even the slightest mistake can lead to structural weakness. Reheating an alloy for rewelding or rebrazing is also a critical process, as it affects the overall strength and integrity of the final product. Finally, process reheating during hot working is essential to maintain the desired properties of the material and can significantly impact the manufacturing outcome (Donachie, 2002).

CHAPTER THREE
SELF PROPAGATING HIGH TEMPERATURES SYNTHESIS (SHS)

Self-propagating high-temperature synthesis (SHS) is an innovative method of synthesizing materials that relies on an external effect to ignite starting reagents. The resulting reaction is highly exothermic and propagates as a solid wave throughout the mixture. This remarkable process is known by names such as gasless combustion, combustion synthesis, self-propagating combustion, and self-propagating exothermic reactions (Subrahmanyam,1992).

SHS has numerous applications in various fields, including materials science, chemistry, and engineering. For instance, it has been used to synthesize metal powders, ceramics, and composites with unique properties. Additionally, the simplicity and cost-effectiveness of SHS make it an attractive alternative to conventional synthesis methods. Over the past 50 years, a wide range of metal alloys, structural ceramics, intermetallic compounds, and composite materials have been produced using SHS techniques in both normal atmospheric conditions and controlled environments such as inert, vacuum, high or low pressure, or even artificial gravity conditions (Alkan, 2015).

The SHS process is characterized by a short processing time, low initiation energy requirement, and ease of operation (Akkas,2010). The simplicity and energy efficiency of this process are due to the absence of complicated experimental configurations and the fact that no additional energy is required once the process is initiated. The elevated temperatures that occur during the combustion wave lead to a greater purity of the products. As the wave moves through the sample, any volatile impurities are expected to be expelled. Any exceptions to this are believed to have been introduced during subsequent product handling, such as grinding, prior to analysis. Metastable phases can form due to the high thermal gradients and rapid cooling rates during combustion (Munir,1989).

The process of synthesizing starts when the combustion wave reaches the heat release zone in a structure that is not in equilibrium or the synthesis zone in a structure that is in equilibrium (Alkan, 2015).

During the reaction known as SHS, the temperature can reach incredibly high temperatures of up to 4000 °C. The velocity of the combustion wave can vary between 0.1-15.0 cm/s, and the heating rate can be as high as 10^6 °C/s (Alkan, 2015).

There are two approaches used in SHS technology. The first way to approach the production process is the producing intermediate products that can be used as raw materials for further processing. Another approach is producing finished products, combining synthesis, structuring, and shaping all in one stage. Figure 3.1 overviews the simplified schematic for the self-propagating high-temperature synthesis process (Mossino,2004).

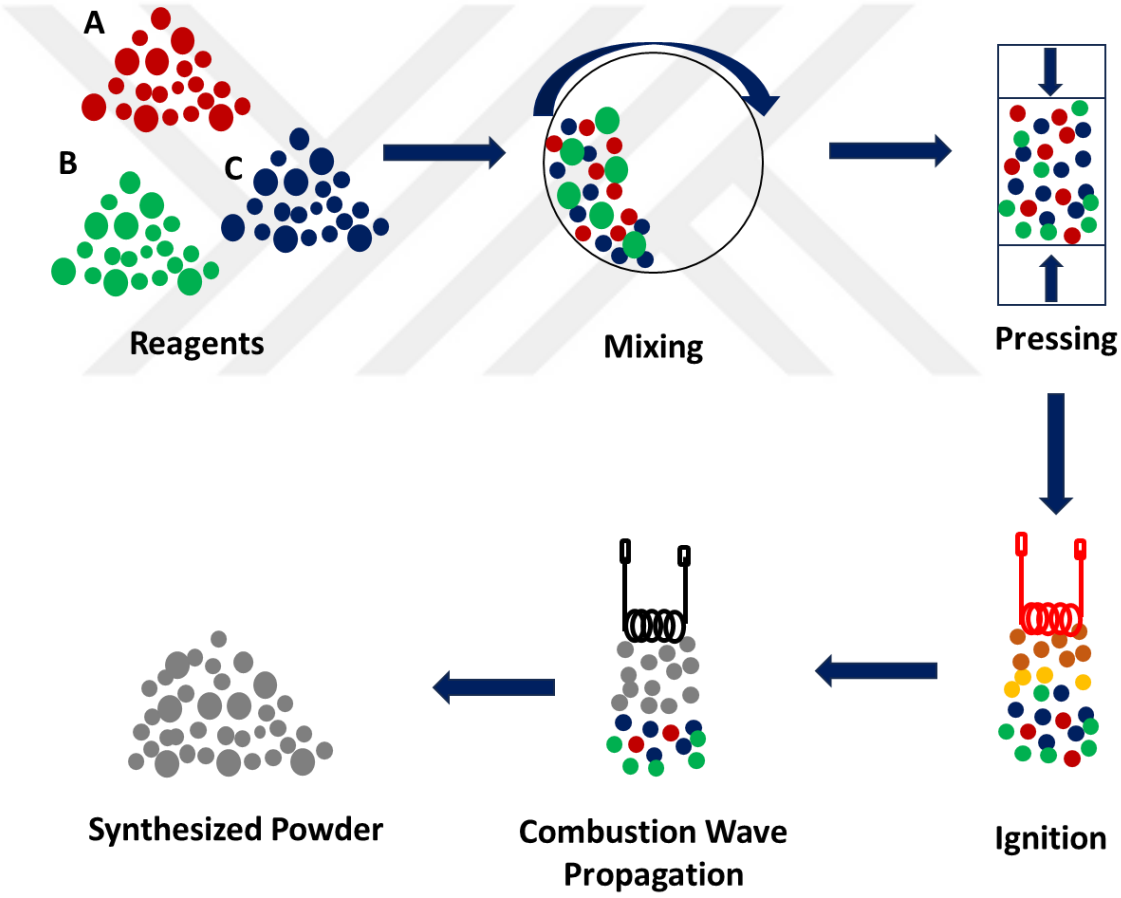

Figure 3.1 The schematic for the self-propagating high-temperature synthesis process (Minasyan,2020)

Over 500 compounds have been successfully synthesized by the SHS method. These materials have found various applications in different fields. Firstly, they are used as abrasives, cutting tools, and polishing powders. These materials are preferred due to their high strength and wear resistance properties. Secondly, resistive heating elements are another application of these synthesized materials. Resistive heating elements are used for various purposes, such as heating liquids, gases, and solids. Shape-memory alloys are another class of materials synthesized by the SHS method. These alloys can regain their original shape after being deformed. They are used in various applications, such as medical devices, aerospace, and automotive industries. In addition, high-temperature intermetallic compounds are another class of materials synthesized by the SHS method. These compounds are used in various applications such as gas turbine engines, aerospace, and automotive industries (Mossino,2004).

They can be used for various purposes, such as producing ceramics for electronic devices and biomedical applications. Lastly, thin film and coatings are another application of these synthesized materials. These films and coatings are used in various applications, such as optical coatings, protective coatings, and semiconductor devices (Mossino,2004).

According to Merzhanov, the physicochemical mechanisms of SHS are:

An important factor to consider in SHS reactions is the adiabatic temperature, Tad. The products reach this temperature due to heat release during a chemical reaction under adiabatic conditions. Merzhanov developed a physicochemical classification of SHS mechanisms for a binary system, which considers the reactants' adiabatic temperatures, melting points, and boiling points. If the temperature at which the reaction is carried out is lower than the boiling point of both elements taking part in the reaction, there will be no vapor phase during the reaction (Subrahmanyam,1992).

Achieving combustion, which is free of ideal gases, can only happen when the ratio of the vapor pressure at the adiabatic temperature to the atmospheric pressure approaches zero. When the temperature of the reaction mixture increases adiabatically and becomes higher than the melting point of the reactants but remains below the boiling point, the reaction proceeds in the liquid phase (Subrahmanyam,1992).

If the adiabatic temperature falls within the melting points of the components, the molten component spreads quickly in the compact, leading to the highest combustion velocity. Table 3.1 provides a classification of reaction mechanisms in two-component systems within SHS based on physicochemical principles (Subrahmanyam,1992).

Complete solid-state combustion occurs when the melting points of the reactants are lower than the adiabatic temperature, resulting in slower combustion velocities. This classification only applies to two-component systems, and the physical state of the resulting product is ignored in the mechanisms. However, understanding the adiabatic temperature and the physico-chemical state of the reactants provides a sufficient basis for envisioning potential reaction mechanisms (Subrahmanyam,1992).

Table 3.1 Classification SHS reaction mechanisms in two-component systems using physicochemical principles (Subrahmanyam,1992)

Relation Between T_{ad}, T_m and T_b	**Characteristics of the system**	**Some Examples**
$T_{ad} < T^{i}_{b}$ $i=1,2$	Free combustion of an ideal gas occurs.	Ti + 2B=TiB_2 T_{ad}=3200 K
$T^{i}_{m} < T_{ad} < T^{i}_{b}$ $i=1,2$	Both components in liquid state	Ni + Al=NiAl T_{ad}=1910 K
$T^{1}_{m} < T_{ad} < T^{2}m$	Solid + liquid reaction.Highest propagation velocity	Ti + C=TiC T_{ad}=3200 K
$T_{ad} < T^{i}_{m}$ $i=1,2$	Both components are in a solid state, which results in a lower combustion velocity and makes combustion more difficult.	2Ta + C = Ta_2C T_{ad}=2600 K
$T^{1}_{b} < T_{ad} < T^{2}_{b}$	One component is in the gaseous phase and the other is in a condensed state. This is a commonly used process.	The creation of nitrides, hydrides, sulfides, selenides, phosphides, and other such substances.
$T_{ad} > T^{i}_{b}$ $i=1,2$	Both reactants in gas phase and solid product	Very few systems studied. Mg + S

3.1 Main Reaction Parameters of SHS

The success of self-propagating high-temperature synthesis (SHS) reactions depends on several variables. These variables include particle size, stoichiometry of reactants, size of pellets, green density, and ignition mode. Each of these factors can play a critical role in the combustion process and affect the outcome of the reaction (Mossino, 2004).

3.1.1 Impact of particle size

The size of the reactant powder has a significant impact on the SHS process. The dimensions of the reactant particles affect the level of completion of the reaction, the temporal sequence, the temperature profile of the combustion zone, and the velocity of the combustion wave. In order to understand the relationship between wave velocity and particle size, it is necessary to incorporate a clear expression of the rate of the SHS reaction into the Fourier heat balance equation (3.1) (Mossino, 2004).

$$k\frac{\partial^2 T}{\partial x^2} - C_p\rho\frac{\partial T}{\partial x} + Q\frac{\partial \eta}{\partial t} = 0 \tag{3.1}$$

Where; k: thermal conductivity, Cp: heat capacity, ρ: density, Q: heat of the reaction α: degree of advancement of the reaction, T: temperature, t: time, x: axis of wave propagation (Mossino, 2004).

3.1.2 Pressing of green powders

The compaction of raw materials is essential for combustion synthesis reactions. The compactness of the system depends on the properties of the materials, such as their hardness and strength. Particles that are less hard will compact more easily. In general, larger particles tend to result in higher packing density and exhibit higher density at all levels of compaction pressure. Conversely, smaller particles are more difficult to compact. A wide particle size distribution can enhance density at any compaction pressure. Powder compacts with considerably high or low densities can be challenging to ignite (Mossino, 2004).

The correlation between the density of green material and the ignition and propagation of the reaction is impacted by the equilibrium of particle contact and heat dissipation from the reaction area, which is determined by the thermal conductivity (Mossino, 2004).

The capillary spreading is also affected by the porosity of the sample. The optimal result of capillary spreading is achieved when the molten phase fills all the empty spaces in the sample. Hence, the sample's optimal density is achieved when the pore volume matches the volume of molten metal. In cases where the metal volume fraction is low, the pores are incompletely filled, leading to reduced interaction between the reactants (Mossino, 2004).

On the other hand, when the metal volume fraction is high, there is excess liquid that fills beyond what is necessary to fill the pores. In either case, the reaction intensity is reduced, which results in an expected decrease in the combustion temperature. The ideal relative density can be calculated by equating the volume of the molten metal and voids in the sample (Mossino, 2004).

3.1.3 Evolution of gaseous substances

There is a possibility of impurities present on the surface of particles in green compact, which can cause the release of gaseous species. These gaseous species can create structural imperfections in the final product due to high combustion temperatures, such as voids, or even complete destruction by explosion. The rapid increase in the amount of gas attracted to the reactant particles and the trapped gas in the spaces between the particles is the main reason the product becomes more fragmented and can even explode (Mossino, 2004).

3.1.4 Calculation of the reactants

Having the correct ratio of the reactants is a crucial parameter in the process. It is worth noting that even a slight deviation from this balance can decrease adiabatic temperature. Excessing either reactants or products in a reaction can decrease its exothermicity, which in turn causes a reduction in the adiabatic temperature due to less heat being released (Mossino, 2004).

Maintaining the proper balance of reactants and products is important to ensure that the reaction proceeds and achieves the desired temperature (Mossino, 2004).

To manage the reaction process and lower the adiabatic temperature, extra product may be used as a diluent. This approach helps to reduce the intensity of the reaction (Mossino, 2004).

3.1.5 Ignition Mode

There are several methods to initiate self-propagating high-temperature synthesis (SHS) reactions. The igniter typically involves a tungsten wire that is heated via electric discharge and used to ignite the mixture directly. Different components can be added to the sample to ignite an exothermic reaction. To standardize ignition conditions for each reaction, radiant flux can be used. This ignition method involves various techniques to initiate combustion synthesis reactions. A radiation source, reflector, and shutter regulate the radiation. Alternatively, a laser can be directed at the sample, generating high heat and igniting it. Another approach is chemical ignition, exposing reactive gases or liquids to green powders. This generates enough heat at the contact surface to initiate the reaction. In addition, microwave energy can be used to initiate combustion synthesis reactions. This technique propagates the reaction from the center of the green pellets to the surface, resulting in a more uniform and controlled ignition. Alternatively, the entire sample can be heated constantly to achieve simultaneous combustion (Mossino, 2004).

CHAPTER FOUR
LITERATURE REVIEW

4.1 Production with SHS

Alkan et al. conducted a study on obtaining low-cost Ni-based superalloy material using the self-propagating high-temperature synthesis (SHS) method under both normal gravity conditions (a = 9.81 m/s^2) and high gravity conditions (up to 1000 g). Al was added to the Co_3O_4-NiO powder mixture as a reducing agent. For normal gravity, a copper crucible was used, and for high gravity, a composite crucible was used. Thermodynamic studies suggest that NiO can be reduced to Ni more easily than Co_3O_4 can be reduced to Co. The addition of alumina slowed down the reaction, decreased the adiabatic temperature, and reduced metal loss. Increasing gravity speed facilitated the separation of products from the slag (Alkan,2015).

The SHS method was utilized by Shekari et al. to produce a NiAl alloy. To do this, they mixed 99.9% pure Al and 99.9% pure Ni powders in a 1:1 ratio before compressing them into various diameters. The temperatures recorded during the study exceeded 2000 K, suggesting that the heat generated was enough to cause the NiAl product (1911 K) to melt. Using the induction-activated self-propagating high-temperature synthesis (SHS) method, a high-density NiAl intermetallic compound was successfully produced. Compared to traditional methods of NiAl production, such as casting and powder metallurgy, this method is fast and efficient while requiring relatively simple and inexpensive equipment. The study also discovered that quick preheating of the sample and the start of the reaction in Ni + Al samples can be achieved through high heating rates. The system temperature often exceeds the melting point of NiAl, resulting in a glossy appearance and good density of the product's cross-sectional surface. This study did not encounter high porosity, which is a major disadvantage of SHS products (Shekari,2017).

The goal of Kılıç's study is to create functionally graded materials (FGM) made of NiTi/NiAl/Ni3Al intermetallics using the self-propagating high-temperature synthesis (SHS) method and to analyze the microstructures of the resulting materials. The study found that an FGM can be produced with the SHS method using different layers, a compacting pressure of 150 MPa, and preheating temperatures of 200-300-400 °C. The samples were then sintered at 1000 °C for 1 hour. Analysis showed that the samples contained pores, combustion chambers, and dendritic formations. The NiTi and NiTi-NiAl regions exhibited the highest hardnesses in the microhardness tests. Therefore, the study concludes that the SHS method can successfully produce an intermetallic FGM consisting of three different layers with different melting temperatures. Increasing preheating temperatures led to a more homogeneous distribution of pores without compromising the sample's integrity (Kılıç,2015).

4.2 Coating Apllications with SHS

In Mohammadkhani et al.'s study, they applied a FeAl coating onto a low alloy steel substrate using the self-propagating high-temperature synthesis (SHS) method. Ni and Al powders with a purity of 99.9% and mixed in equal molar ratios were compressed using a uniaxial cold press under 150 MPa of pressure and placed onto the substrate inside a 950 °C oven (Mohammadkhani,2016).

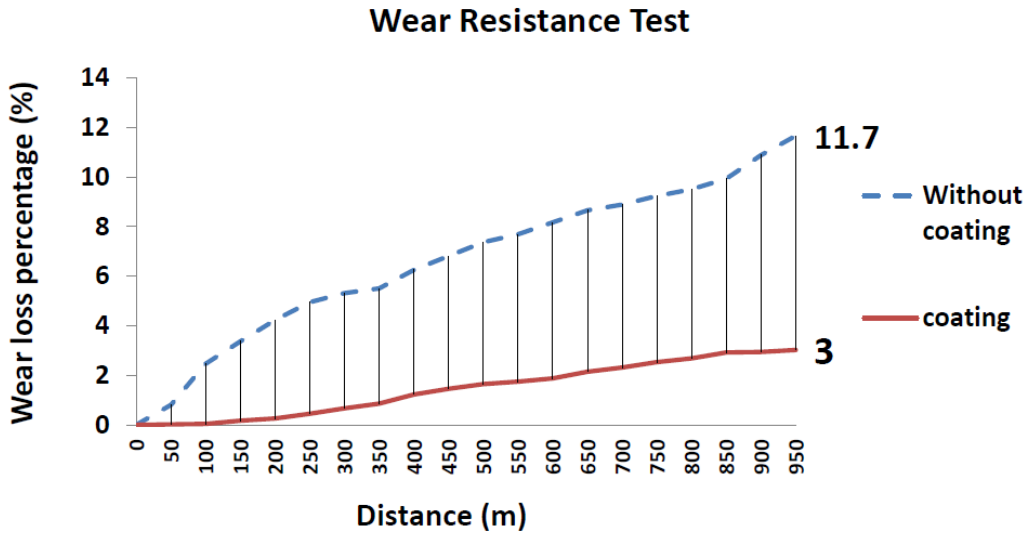

Figure 4.1 Comparison of wear resistances of coated and uncoated specimens. (Mohammadkhani,2016)

The abrasion resistances of both the coating and the substrate were measured using the pin-on-disc abrasion test, which revealed that the SHS reactions at high temperatures were effective in coating the substrate. Furthermore, the tribological properties of the coated samples were significantly improved which shows that Figure 4.1, resulting in a 4-fold increase in wear and corrosion resistance compared to bare steel (Mohammadkhani,2016).

Li et al. conducted a study on the interface and microstructures that were formed by SHS welding of SiC ceramic and Ni-based superalloys. The starting metallic material used for welding was the Ni-based superalloy. The welding materials (fillers) used and their purities are as follows: Ti powder (99.23 wt%), Ni powder (99.7 wt%), and Al powder (99.6 wt%). C powder was also utilized as a component in welding materials. The SiC ceramic billet, powder compact, and Ni-based superalloy billet were placed in a graphite die. Then, a pressure-aided SHS welding test was conducted. The metal powder mixtures in different compositions were used. Every filler reached a successful welding point except one. It has been observed that the filler has a high C content. This may result in the formation of stable TiC due to the reaction of C with the active component Ti, leading to a reduction in the active component. Additionally, the presence of TiC may hinder the mobility of the remaining active components, lowering the chances of contact between the SiC ceramic and active components (Li,2000)

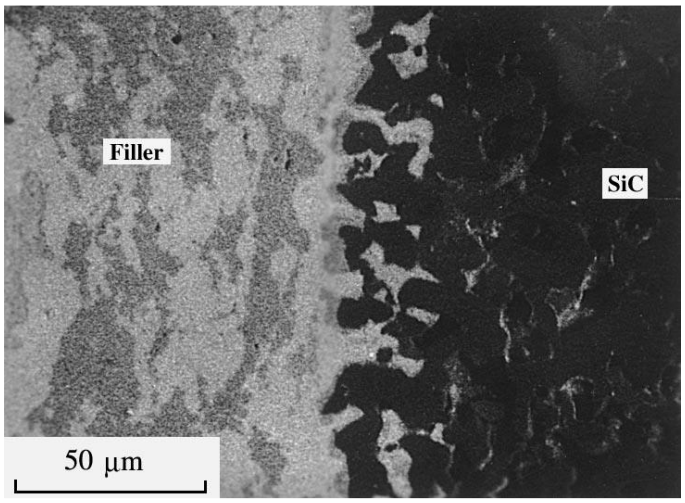

Figure 4.2 SEM micrograph of the interface of SiC ceramic/reaction products of filler No. SS-2 (Li,2000)

When the results are examined, excellent bonding exists at the interfaces within the total welded area (Figure 4.2). The molten metal can enter the exposed pores of the ceramic material and create a mechanical connection between the ceramic and the reaction products once it solidifies (Li,2000).

Shchukin et al. showed that it is possible to bond an intermetallic compound NiAl coating to a Mo substrate using the self-propagating high-temperature synthesis (SHS) method without melting the Mo substrate. This process is also known as SHS welding. In the experiments, they used the Mo substrates as foils with a thickness of 120 μm, a Ni powder, and an Al powder. The equimolar mixture of Ni and Al powder, with a 20 mm diameter and 10 mm height, was compacted onto a Mo substrate and placed on one or both sides. The SHS process was then conducted in the presence of air. The combustion process began by applying an electrically heated graphite tape. This caused a strong welded joint to form between the Mo foil and the NiAl coating in the (Ni + Al)/Mo-substrate sample due to the SHS reaction (Figure 4.3). (Shchukin,2019).

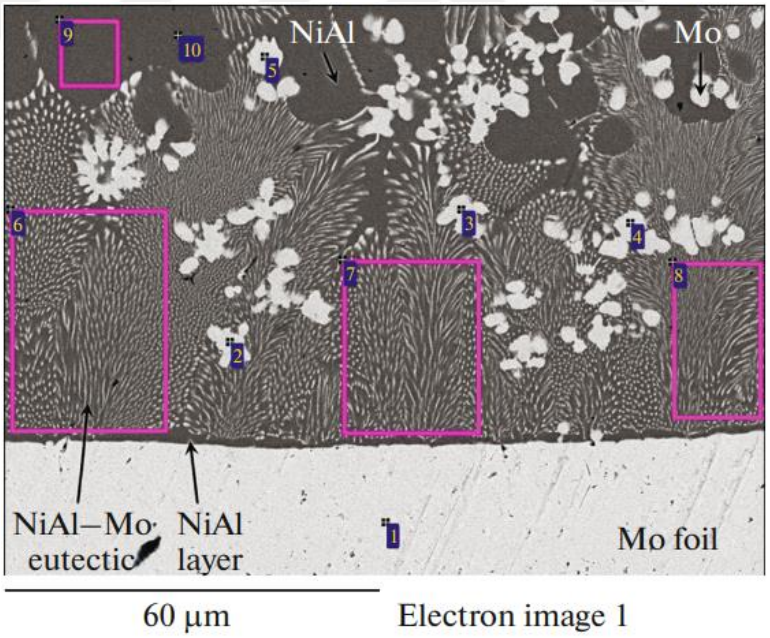

Figure 4.3 The microstructure between the Mo substrate and NiAl coating (Shchukin,2019)

The study discovered that the microhardness of the Mo/NiAl transition layer is higher (2860 MPa) compared to the welded NiAl coating (2360 MPa) and the Mo substrate (1830–1990 MPa) (Shchukin, 2019).

This shows that the NiAl intermetallic compound has been strengthened due to Mo dissolving in it and the creation of a NiAl-Mo eutectic, as well as the formation of Mo nano-precipitates in the NiAl dendrites (Shchukin, 2019).

Systschev et al. conducted a study on joining NiAl to Ni substrates using a load-assisted SHS reaction. The study examined the bonding process between the liquid reaction products and the Ni substrate. In that study, commercial elemental powders of Al and Ni were used as starting materials and substrates of Ni. The metal powders were mixed homogeneously and pelleted. Next, a Ni disk (substrate) was positioned onto a Ni-Al green compact and ignited using an acetylene burner. After combustion was completed, a load of 2 tons was applied to the still-hot NiAl, a product of the SHS reaction, using a press machine (Systschev,2013).

The joining process was carried out in the air. As a result, the interfacial joint contained the following phases: $AlNi_3$, AlNi, Al_3Ni_5, Al_3Ni_2, and Ni. The high-temperature melt formed in the Ni-Al layer due to the heat effect of the SHS reaction plays a significant role in regulating the SHS joining process. The porosity of the resulting seam was discovered to be influenced by the preheating temperature and the applied force (Systschev,2013).

CHAPTER FIVE
EXPERIMENTAL STUDIES

In this study, an AISI 1050 steel was selected as the substrate material, while Inconel 718 superalloy was chosen as the coating material due to its superior properties. The production of the selected superalloy was realized by applying of SHS reaction. The diameters of the substrate, the weight of starting mix, and the experimental setup were investigated. The SHS experiments were conducted using three distinct setups. These setups are explained in detail in the following section. This section is once again divided into three headings. These are; the preparation stage before the experiment, SHS experiments, and characterization studies.

5.1 Preparation Stage Before the Experiment

5.1.1 Preparation of Substrates

The steel bar with a diameter of 20 mm was cut into pieces with a height of 10 mm, and the weight of each piece was measured. The pieces were ground and polished using sandpaper with 80, 240, 400, and 800 grits. The PRESI MECAPOL P 230 Grinding-Polishing device was used for the process. A water-based 3-micron single-crystal diamond paste supplied by Metkon Company was applied during polishing.

5.1.2 Preparation of Initial Mixtures

The composition of superalloys (specifically Inconel 718) and the necessary amounts of raw materials were determined using the HSC Chemistry program. The value of T_{ad} was once again calculated as 2952,6 K using the HSC Chemistry program. Table 5.1 below presents the calculated components of the alloy and the amounts of raw materials used in the experiment. The metal oxide powders (min. 98.0 % purity and 100-150 μm particle size) were dried in the oven at 100°C for a minimum of 2 hours to eliminate any moisture. After weighing 50 g and 100 g on a precision scale, the raw material powder mixture was placed in a plastic box and mixed in an Emor brand powder mixer at 500 rpm for 30 minutes.

Table 5.1 Calculated Inconel 718 compositions and amounts of raw materials used in experiments

Calculated alloy compositions (mass %)							**Weight of raw materials (g)**								
Ni	Cr	Nb	Mo	Ti	Co	Fe	NiO	Cr_2O_3	Nb_2O_5	MoO_3	TiO_2	Co_3O_4	Fe_2O_3	Al	**Total**
52	21	6	4	3	2	12	18,66	8,66	2,43	1,69	1,42	0,77	4,84	11,53	**50**
52	21	6	4	3	2	12	37,34	17,32	4,85	3,38	2,83	1,54	9,69	23,05	**100**

5.2 SHS Experiment

5.2.1 First Experimental Setup

As mentioned earlier, SHS experiments were performed using three different setups. For the first setup, a copper crucible was chosen (h = 140 mm, d_{in} = Ø 40 mm, d_{out} = Ø 50 mm), along with a steel substrate underneath it. The substrate surroundings were left empty and filled with either alumina (Al_2O_3) or an exothermic sleeve. This process was repeated for the substrates, with a diameter of 20 and 40. The schematic view of the experimental setup for the first synthesis is given in Figure 5.1. The decision to use a copper crucible was based on its high thermal conductivity, which helps to distribute heat evenly throughout the mixture during the reaction.

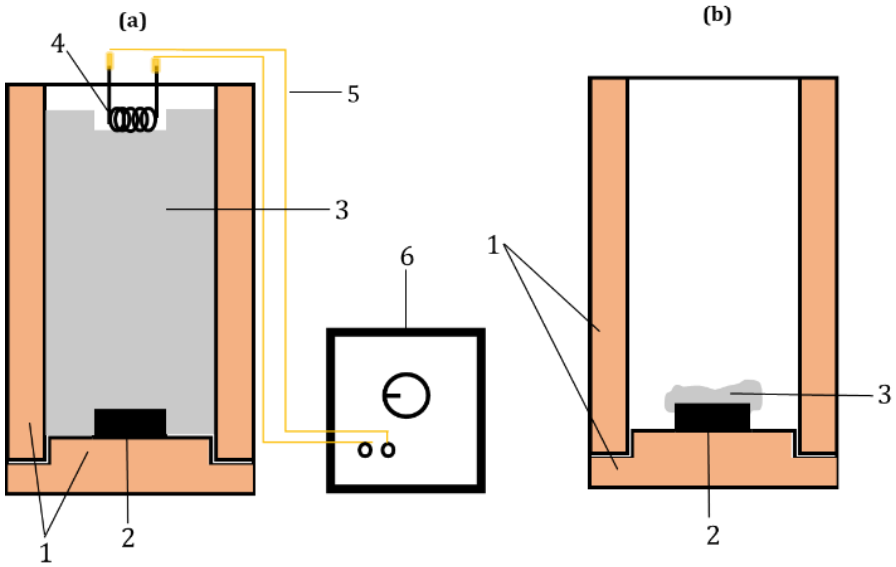

Figure 5.1 The schematic view of SHS experimental setup for the first synthesis (a) before combustion (b) after combustion (1) Cu crucible, (2) steel substrate (3) powder mixture, (4) igniter, (5) Cu cable, (6) power supply.

The starting mixture was then directly charged into the crucible, consisting of a carefully measured amount of reactants. To initiate the reaction, a resistance wire ($Cr_{25}Al_5$) was selected with current flowing through it, which was then placed on top of the crucible to provide heat. The wire was carefully positioned to ensure that it was in direct contact with the mixture and that the heat generated by the wire was evenly distributed throughout the crucible. Once the combustion was complete, the wire was removed from the system. When SHS reactions were finished, the metal and slag were acquired by quickly cooling the crucible in water. The resulting products were then analyzed.

5.2.2 Second Experimental Setup

The experimental setup consisted of two crucibles placed on a steel substrate. In order to prevent direct contact between the starting mixture and the substrate, aluminum foil was placed between the crucibles. The starting mixture was then placed on top of the foil. Ignition was initiated by using a resistance wire ($Cr_{25}Al_5$). When the reaction started, the molten metal was expected to flow onto the steel substrate. Figure 5.2 shows the schematic view of the experimental setup used for the second synthesis.

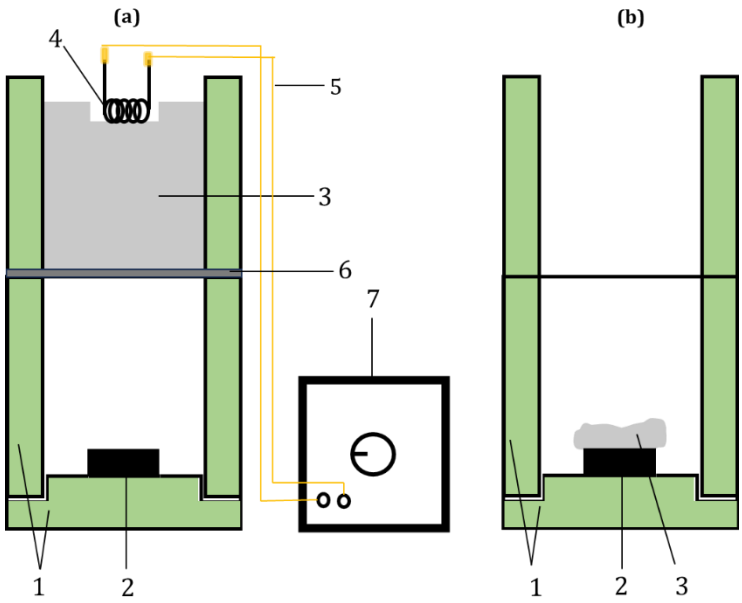

Figure 5.2 The schematic view of SHS experimental setup for the second synthesis (a) before combustion (b) after combustion (1) Cu crucible, (2) steel substrate (3) powder mixture, (4) igniter, (5) Cu cable, (6) Al foil, (7) power supply

The surroundings of the substrate were either left empty or filled with alumina (Al_2O_3), similar to the first configuration. This procedure was carried out for both 20 and 40 diameters substrates.

5.2.3 Last Experimental Setup

In contrast to the second configuration, the top crucible in the last setup remained stationary while the bottom crucible rotated at different speeds. The surroundings of the substrate in the lower crucible could not be left empty, so it was filled only with alumina. The decision to keep the upper crucible still while changing the rotation of the lower crucible was deliberate, made to prevent the accumulation of slag that had occurred in previous setups. The schematic view of the last experimental setup is given in Figure 5.3.

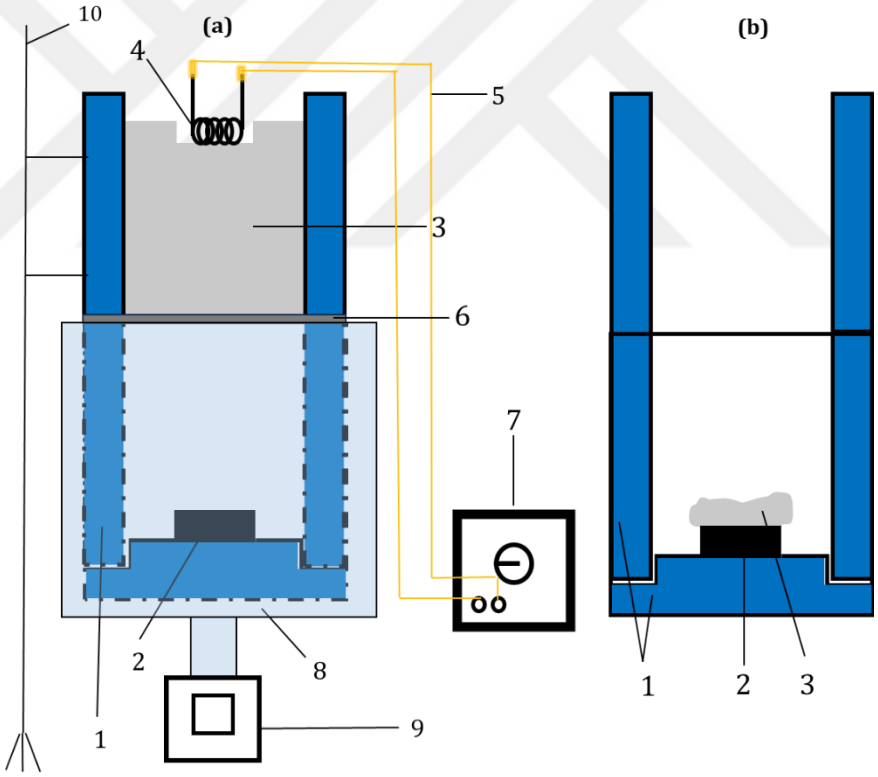

Figure 5.3 The schematic view of the last experimental setup (a) before combustion (b) after combustion (1) Cu crucible, (2) steel substrate (3) powder mixture, (4) igniter, (5) Cu cable, (6)Al foil, (7) power supply, (8) rotator part, (9) mechanical rotator, (10) tripod

Moreover, the variable (200,350,500) Rpm of the spinning crucible demonstrated how different speeds affected the coating, enabling more subtle conclusions to be drawn from the experiment as a whole. After the combustion, the wire was removed from the system. The crucible was quickly cooled in water to acquire the metal and slag from the SHS reactions. Finally, the resulting products were analyzed.

During the initial setup, it was noticed that the height of the substrate had decreased. This was because the adiabatic temperature of the starting mixture containing 100 g was higher than that of the one containing 50 g. As a result, the starting mixture was weighed at only 50 g for the second and third setups.

5.3 Characterization Studies

The characterization studies involved investigating chemical analysis, microstructure analysis, and mechanical properties. An X-ray fluorescence device was used to perform the chemical analysis of the Inconel 718. The microstructures of the products were examined using ZEISS Gemini 560 and Evo MA10 SEM (Scanning Electron Microscope) devices equipped with an EDS (Energy Dispersive Spectrometer). To analyze the microstructures, the samples were ground using sandpaper with grit sizes of 80, 240, 400, 800, and 1200, respectively, and then polished using the PRESI MECAPOL P 230 Grinding and Polishing device. A water-based 3-micron single-crystal diamond paste supplied by Metkon Company was used for polishing. The mechanical properties were analyzed using the Shimadzu HMV-2 microhardness (micro-Vickers) device. A load of 0.5 kg was applied to each sample, and six different values were taken to ensure a comprehensive analysis. Specifically, two values were taken from the coating part of the sample, and an additional two values were taken from the substrate. Then, one value was measured from the interphase near the coating and another from the interphase close to the substrate.

CHAPTER SIX
RESULTS AND DISCUSSIONS

When reviewing the experimental studies, it becomes clear that three different mechanisms were utilized for the following reasons:

-The initial setup process is straightforward. However, it was observed that there was some slag present in certain areas between the coating and substrate despite the use of aluminum as the reductant during direct charging of the starting mixture.

-The second mechanism was established to prevent slags from accumulating on the interface. This involved planning for the starting mixture to flow in its molten form rather than as a direct charge on the surface of the substrate.

- During the second setup, it was noted that the molten metal was only flowing toward a specific part of the steel substrate. As a result, a rotational force was introduced to address this issue. This led to the implementation of the third mechanism, where the crucible is rotated. Table 6.1 displays details of the test parameters and results.

Table 6.1 Details regarding the parameters and results of the test.

SETUP NO.	TEST NO.	ROTATION SPEED of the CRUCIBLE	STEEL SUBSTRATE TYPE	STEEL SUBSTRATE SURROUNDINGS	TYPE of SUPER ALLOY PRODUCED	AMOUNT OF INITIAL MIXTURE	RESULTS
FIRST SETUP	1	Constant	Ø20 SAE 1050	Empty	INCONEL 718	100 g	Slag has accumulated at the interface
	2	Constant	Ø20 SAE 1050	Filled with Al_2O_3	INCONEL 718	50 g	Successful
	3	Constant	Ø20 SAE 1050	Filled with Exothermic Sleeve	INCONEL 718	100 g	The composition of a steel substrate has been mixed with that of a superalloy.
	4	Constant	Ø20 SAE 1050	The substrate surroundings was filled with Al_2O_3 and the top with an exothermic sleeve.	INCONEL 718	50 g	Successful
	5	Constant	Ø40 SAE 1050	Empty	INCONEL 718	50 g	Successful

SECOND SETUP	**6**	Constant	Ø20 SAE 1050	Filled with Al_2O_3	INCONEL 718	50 g	Successful
	7	Constant	Ø40 SAE 1050	Filled with Al_2O_3	INCONEL 718	50 g	Successful
LAST SETUP	**8**	200 Rpm	Ø20 SAE 1050	Filled with Al_2O_3	INCONEL 718	50 g	Successful
	9	350 Rpm	Ø20 SAE 1050	Filled with Al_2O_3	INCONEL 718	50 g	The coating alloy is deposited on the edges of the substrate, rather than on the surface.
	10	500 Rpm	Ø40 SAE 1050	Filled with Al_2O_3	INCONEL 718	50 g	The coating alloy is deposited on the edges of the substrate, rather than on the surface.

Prior to conducting any experiments, the Inconel 718 superalloy bulk, whose composition was determined using the HSC program, was fabricated in the initial experimental setup. The image of the produced IN718 alloy can be seen in Figure 6.1.

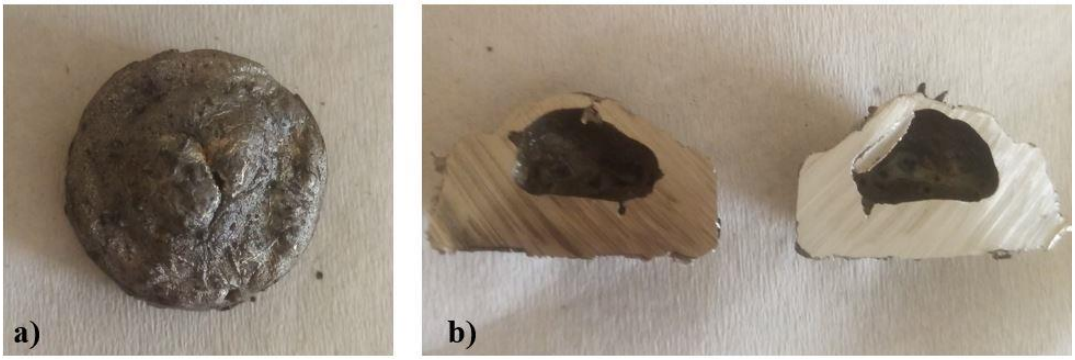

Figure 6.1 Image of IN718 alloy produced by SHS a) Bulk State b) cross-sectional state (Personal archive, 2023)

The XRF results of the coating Inconel 718 were compared with the predicted Inconel 718 alloy in the HSC chemistry program. The results are shown in Table 6.2. The close similarity between the predicted and actual composition of the alloy suggests that the SHS method was a success.

Table 6.2 Comparison between the predicted compositions of Inconel 718 and the results obtained through X-ray fluorescence (XRF).

Preticted Inconel 718 compositions (mass %)							**XRF Results (mass %)**						
Ni	Cr	Nb	Mo	Ti	Co	Fe	Ni	Cr	Nb	Mo	Ti	Co	Fe
52	21	6	4	3	2	12	55,3	17,8	5,62	3,97	0,48	2,19	11,3

6.1 The Results of the Experiments in the First Setup

As indicated in Table 6.1, the initial five experiments were performed using the first setup. In experiment 1, slag accumulated between the steel substrate and the coating. In experiment number 3, the exothermic sleeve increased the adiabatic temperature, causing the steel substrate to melt, and it was observed that the composition of 1050 steel and Inconel 718 super alloy was mixed as a result.

On the other hand, in the test results numbered 2,4,5, a strong bond was formed between the coating and the steel substrate. The strong bond and lack of pores observed at the interface indicate that the self-propagating high-temperature synthesis (SHS) reaction has successfully occurred. Not only production but also coating can be done through self-propagating high-temperature synthesis. (Subrahmanyam, 1992).

SEM and optic microscope photographs of the related experiments are given in Figure 6.2. The results indicate that the superalloy coating effectively penetrated the substrate. Furthermore, the thickness of the coating on these samples was measured and is presented in Figure 6.3. Different thicknesses were observed, including 4 mm, 5 mm, 8 mm, and 9 mm.

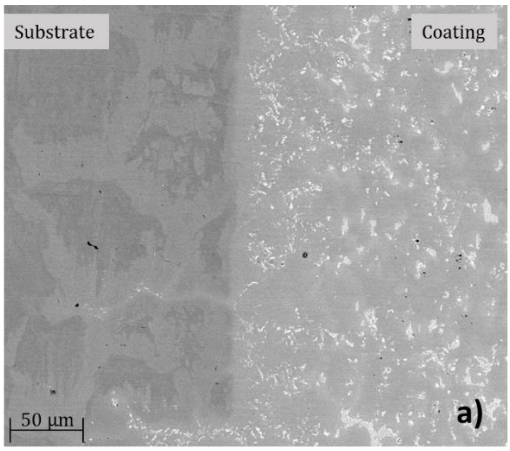

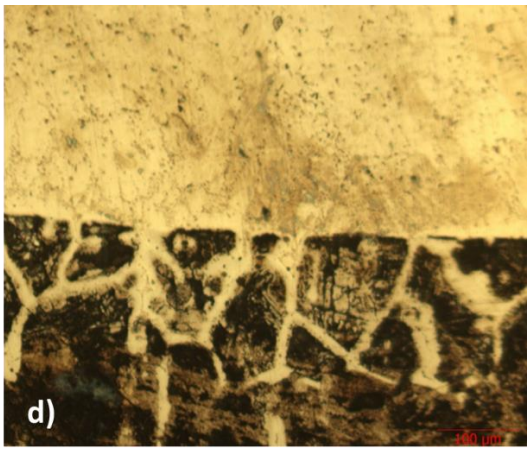

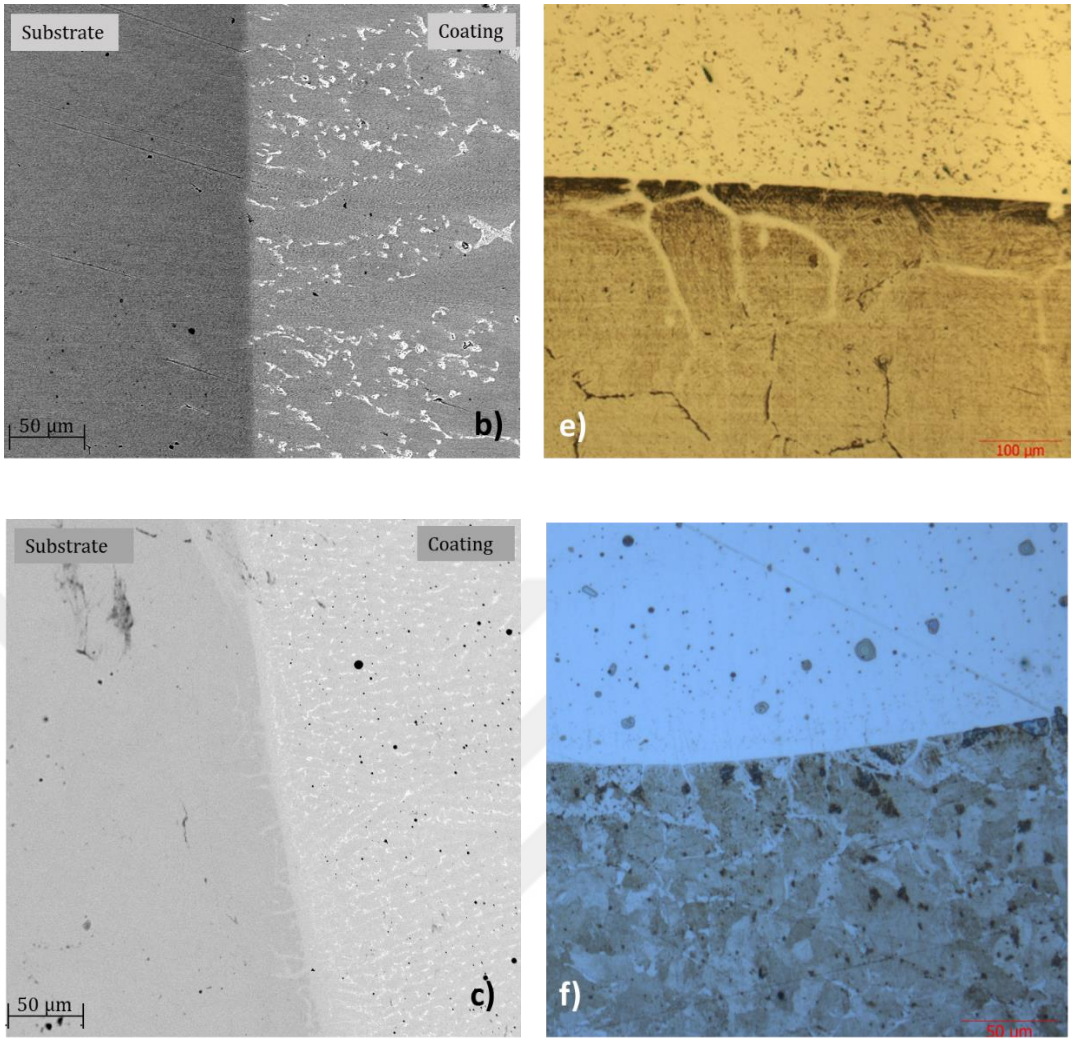

Figure 6.2 SEM and optic microscope photographs of the related experiments a-d) Experiment no:2 b-e) Experiment no:4 c-f) Experiment no:5

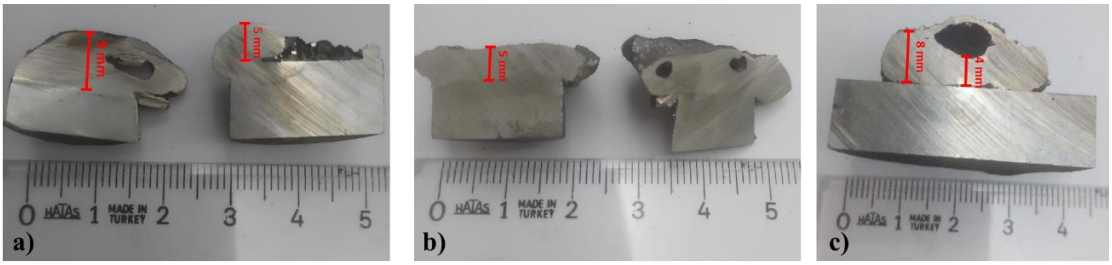

Figure 6.3 Coating thickness measurements of the samples of the first experimental setup a) Experiment no:2 b) Experiment no:4 c) Experiment no:5 (Personal archive, 2023)

The EDS results of the coated samples are presented in Figure 6.4. This figure reveals that various regions of the coated and substrate parts exhibited distinct phase morphology and composition. The distribution of the components of the Inconel 718 superalloy into the steel substrate is remarkable. These findings indicate that the coating process has effectively altered the surface properties of the substrate, resulting in the formation of a material with enhanced mechanical and corrosion resistance properties.

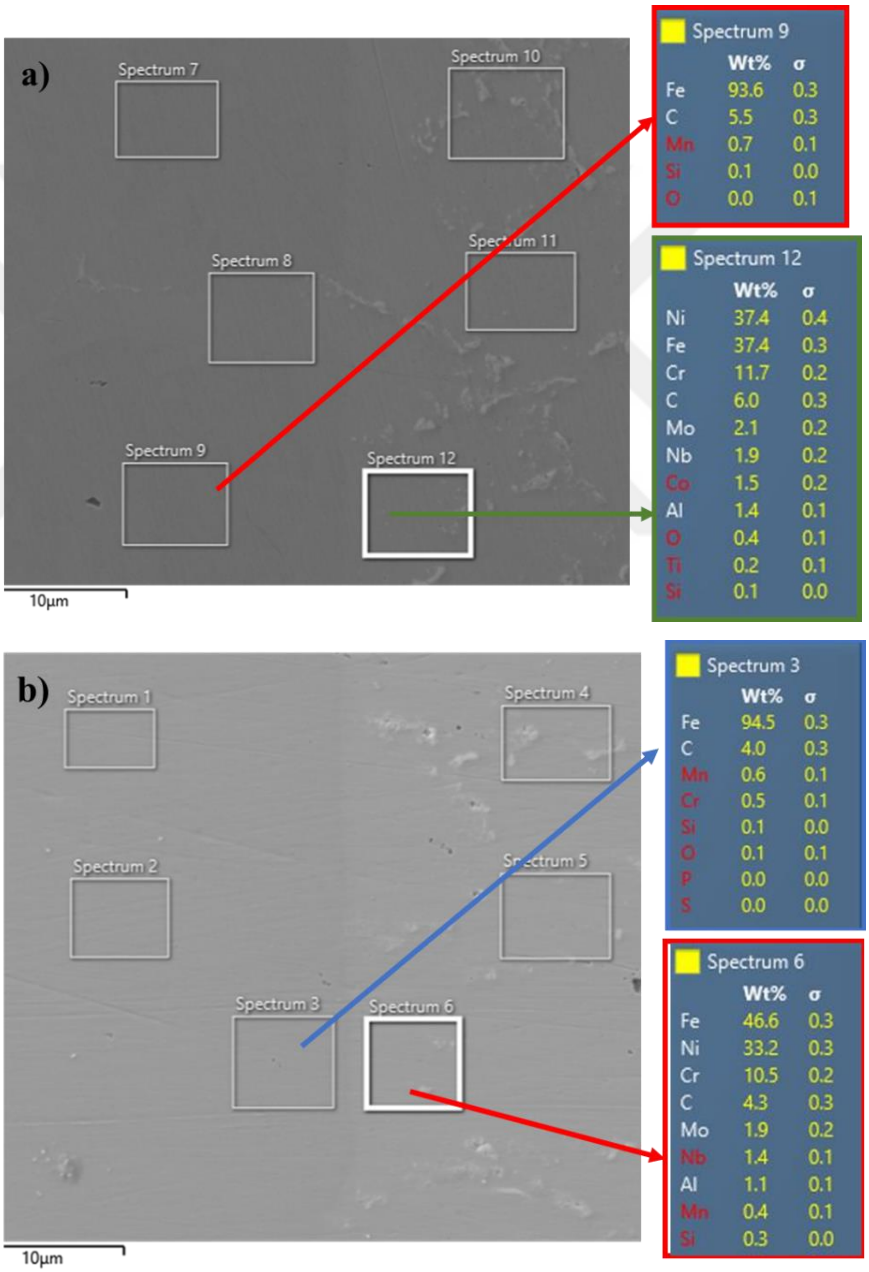

Figure 6.4 The results of the EDS analysis for the coated samples. a) Experiment no:2 b) Experiment no:4

In Figure 6.5, microhardness measurements were taken at the coating portion, the interface, and the steel substrate using a 0,5 kg load. According to the results, the hardness value increased from the steel substrate to the superalloy coating in all three samples.

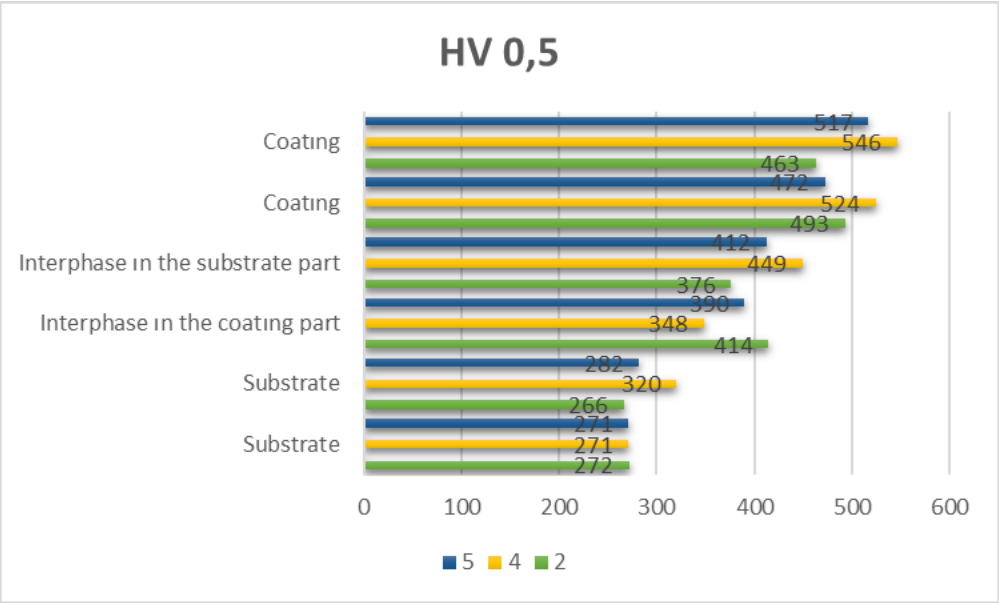

Figure 6.5 Microhardness measurements taken from different regions at first setup' experiments

Upon examination of the interface near the steel substrate, it was observed that the surface properties of the low-alloy steel material had improved. This improvement in surface properties is due to the diffusion of elements from the superalloy coating into the low-alloy steel substrate. The diffusion of these elements results in an increase in the hardness and wear resistance of the steel substrate.

6.2 The Results of the Experiments in the Second Setup

As shown in Table 6.1, experiments 6 and 7 were conducted using the second setup. These experiments were only partially successful, as while the connection was fully formed at the interface, there were also porosities found in the material. Figure 6.6 displays SEM and optic microscope photographs from experiments 6 and 7. Based on the information presented in Figure 6.6(a), it appears that porosities were experienced due to the coating's lack of uniformity.

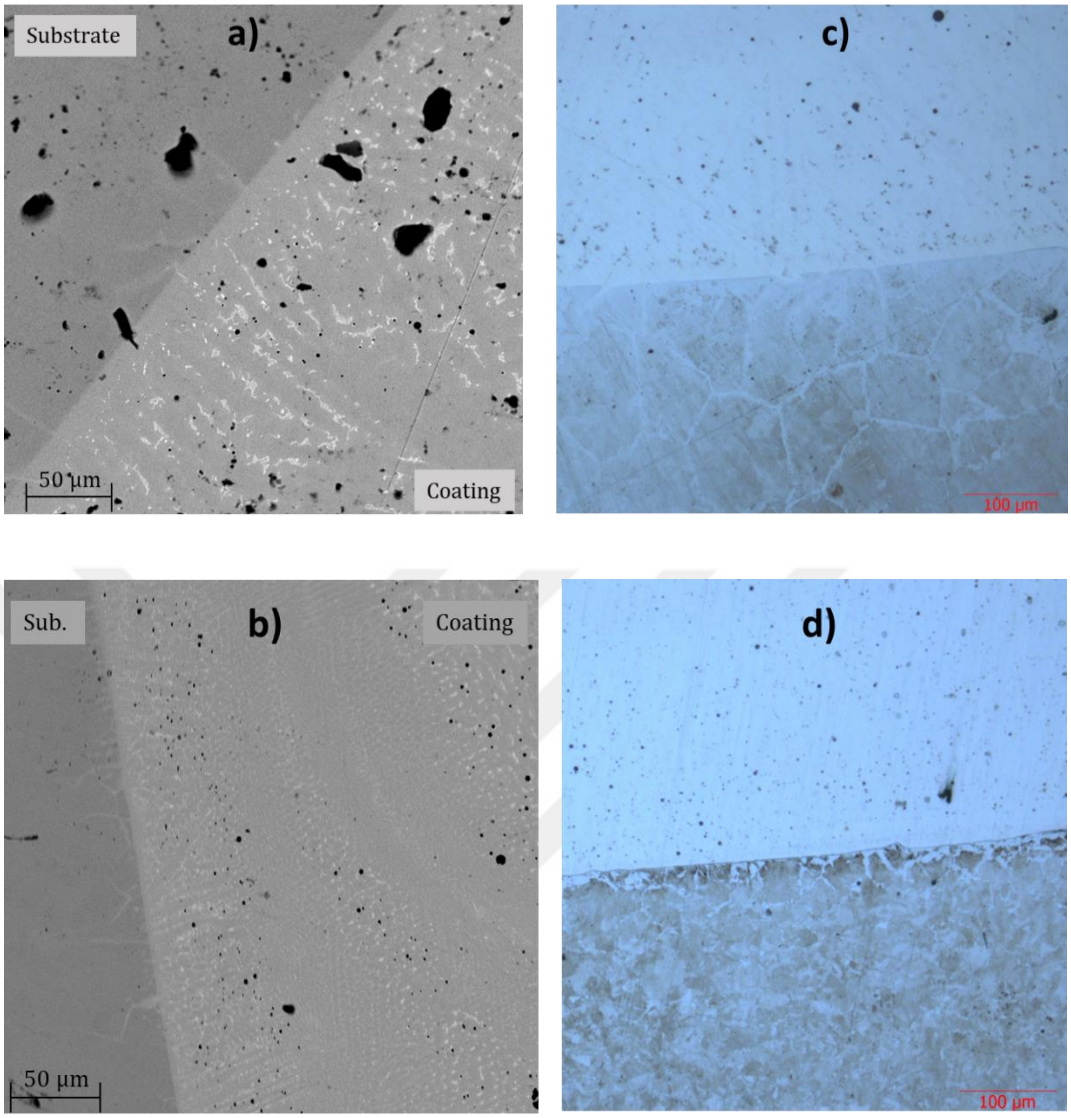

Figure 6.6 SEM and optic microscope photographs from experiments 6(a-c) and 7(b-d)

Figure 6.7 shows the EDS results of the coated samples from Experiments 6. Even though there were porosities, the phase morphology and composition of the coated and substrate segments were different. In the X-ray maps, it can be observed that there were transitions of Ni, Cr, Nb, Mo, and Al towards the steel substrate. Additionally, the matrix of the coating alloy was composed mainly of a nickel-rich (γ) phase, with some Nb-rich phases present in the microstructure. These Nb-rich structures are believed to belong to the γ′′ phase. Furthermore, some eutectic formations were observed in the coating, although in small amounts.

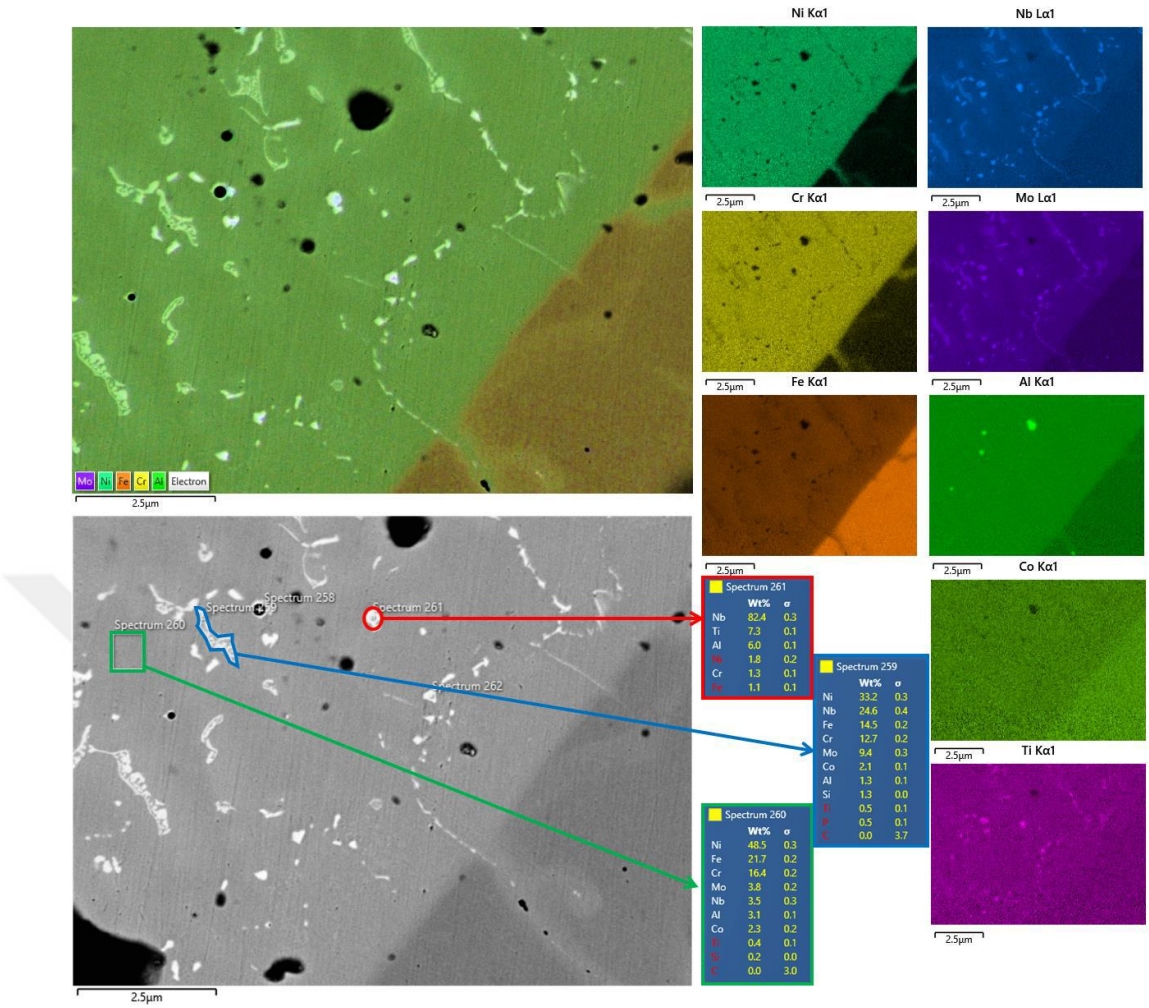

Figure 6.7 The EDS results of the coated samples from Experiments 6

According to the data presented in Figure 6.8, samples 6 and 7 show an increase in material hardness from the steel substrate to the coating. This finding is consistent with the results observed in the initial setup, where similar trends were identified.

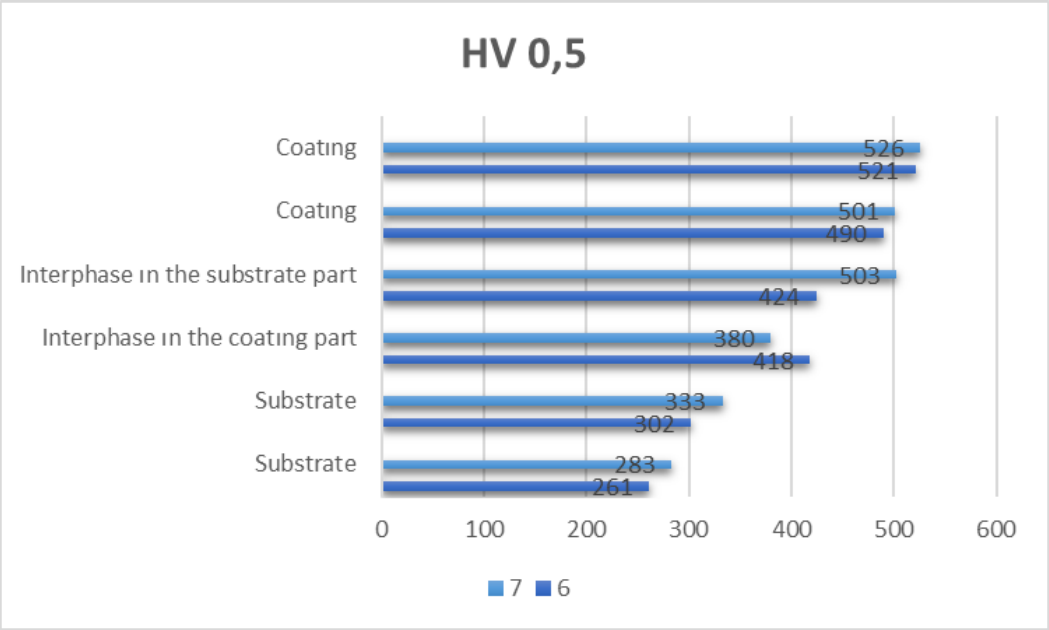

Figure 6.8 Microhardness measurements taken from different regions at second setup' experiments

6.3 The Results of the Experiments in the Last Setup

As noted in Table 6.1, experiments 8, 9, and 10 utilized a rotary system. The rotary system was chosen due to its ability to distribute the molten coating metal across the steel substrate evenly. However, during the experiments, it was observed that increasing the rotation speed had an unintended effect. Instead of evenly distributing the molten coating metal across the surface of the steel substrate, the metal began to accumulate on the edges of the substrate. (Figure 6.9).

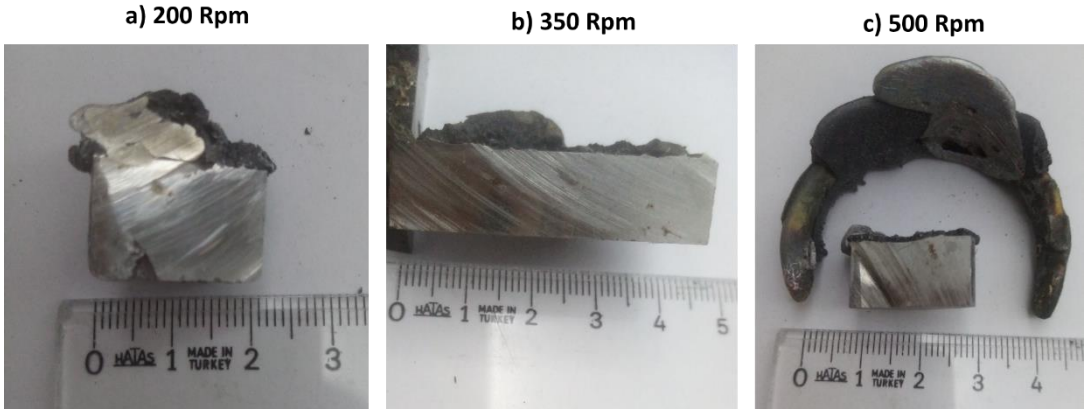

Figure 6.9 The variation in the samples based on their velocity in the cross-section photographs (Personal archive, 2023)

The lowest speed of 200 Rpm produced the best results among the three experiments. The cross-section photographs in Figure 6.9 illustrate the variation in the samples based on their velocity. The SEM photos for the successful Experiment 8 are displayed in Figure 6.10.

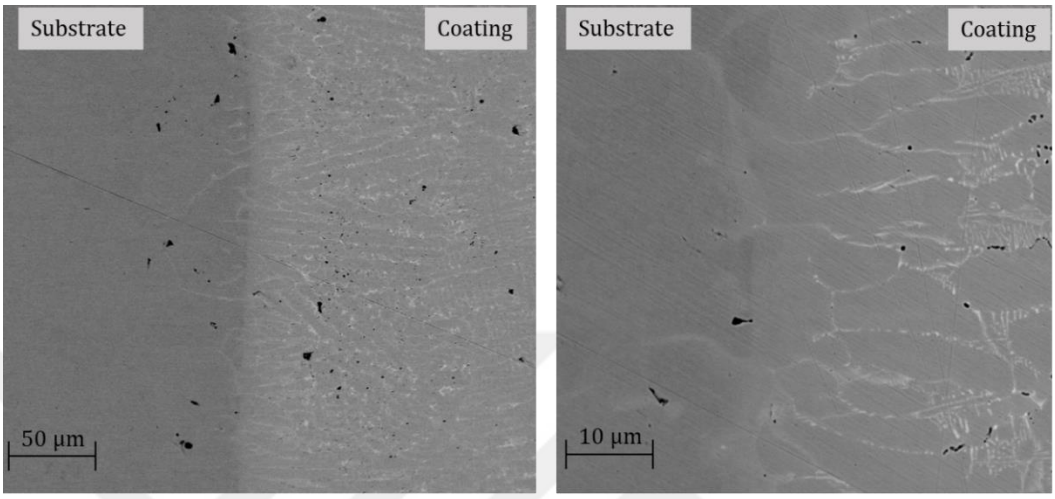

Figure 6.10 Experiment 8 is associated with the SEM photographs.

Upon thorough examination of the SEM results, it was observed that there was a diffusion process that occurred between the surface of the steel substrate and the coating metal at the interface. This diffusion process resulted in the formation of dendritic structures characterized by branching patterns.

CHAPTER SEVEN
CONCLUSIONS

This study utilized the self-propagating high-temperature synthesis (SHS) method, which is a simple, inexpensive, and low-energy way to produce Inconel 718 super alloy using metal oxide powders and reducing metal powder mixtures. The alloy was then directly coated onto low alloy steel substrates using three different mechanisms, and the resulting outcomes were examined. The conclusions drawn from the experimental results presented in this thesis can be summarized as follows:

1- The SHS (Self-propagating High-temperature Synthesis) method is a highly effective and efficient process for producing Inconel 718 alloy, a nickel-based superalloy used in various high-temperature applications. This method is applicable not only to pure metal powders but also to metal oxide powders that are commonly used in the synthesis and coating of other low-alloy steel materials.

2- The SHS method is a process used to produce a coating that exhibits strong bonding properties at the interfaces.

3- The hardness value, which is a measure of a material's resistance to deformation, increased significantly from the steel substrate to the superalloy coating. This suggests that the superalloy coating has improved mechanical properties compared to the low alloy steel substrate. Upon closer examination of the interface between the two materials, it is evident that the surface properties of the low alloy steel material have been enhanced.

4- The concept of having alumina surrounding the steel substrate resulted in a decrease in the adiabatic temperature. However, this reduction was not significant enough to impact the reaction, and, as a result, the substrate did not undergo melting.

5- Unlike alumina, it was found that the exothermic sleeve raised the adiabatic temperature.

6- The increase in rotation speed had an unintended consequence. Instead of uniformly spreading the molten coating metal on the steel substrate's surface, the metal started accumulating on the substrate's edges.

7- There have been numerous studies conducted on the production of new materials and coating on substrates using the SHS method. However, what distinguishes this project is the utilization of affordable metal oxide powders as the initial mixture.

8- One of the advancements introduced by this project is the use of low alloy steel materials, which exhibit reduced working potential at high temperatures. However, their wear and corrosion resistance is significantly enhanced when coated with super alloy material.

9- Superalloys also have various applications and are denser and more costly compared to steel materials. One aspect to consider for enhancement is the reduction of density and cost when utilizing them with steel substrates.

REFERENCES

Akca, E., & Gürsel, A. (2015). A review on superalloys and IN718 nickel-based INCONEL superalloy. *Periodicals of engineering and natural sciences*, *3*(1).

Akkas, B., Alkan, M., Derin, B., & Onüralp, Y. (2011). Production of zirconium diboride powder by self propagating high temperature synthesis. *Advances in Science and Technology*, *63*, 251-256.

Alkan, M., Sonmez, M. S., Derin, B., Yücel, O., Andreev, D. E., Sanin, V. N., & Yukhvid, V. I. (2015). Production of Al-Co-Ni ternary alloys by the SHS method for use in nickel based superalloys manufacturing. *High Temperature Materials and Processes*, *34*(3), 275-283.

ÇAY, V. V., & Sermin, O. Z. A. N. (2005). SÜPERALAŞIMLAR VE UYGULAMA ALANLARI. *Fırat Üniversitesi Doğu Araştırmaları Dergisi*, *3*(2), 178-188.

Donachie, M. J., & Donachie, S. J. (2002). *Superalloys: a technical guide*. ASM international

Gui, W., Zhang, H., Yang, M., Jin, T., Sun, X., & Zheng, Q. (2017). The investigation of carbides evolution in a cobalt-base superalloy at elevated temperature. *Journal of Alloys and Compounds*, *695*, 1271-1278.

Gui, W., Zhang, X., Zhang, H., Sun, X., & Zheng, Q. (2019). Melting of primary carbides in a cobalt-base superalloy. *Journal of Alloys and Compounds*, *787*, 152-157.

Jokisaari, A. M., Naghavi, S. S., Wolverton, C., Voorhees, P. W., & Heinonen, O. G. (2017). Predicting the morphologies of γ precipitates in cobalt-based superalloys. *Acta Materialia*, *141*, 273-284.

KILIÇ, M. (2015). Kendi İlerleyen Yüksek Sıcaklık Sentezi İle Fonksiyonel Derecelendirilmiş İntermetalik Malzemelerin Üretimi ve Mikroyapılarının İncelenmesi. *Journal of Life Sciences*, *5*(2).

Kracke, A., & Allvac, A. (2010, October). Superalloys, the most successful alloy system of modern times-past, present and future. In *Proceedings of the 7th International Symposium on Superalloy* (Vol. 718, pp. 13-50).

Li, S., Duan, H., Liu, S., Zhang, Y., Dang, Z., Zhang, Y., & Wu, C. (2000). Interdiffusion involved in SHS welding of SiC ceramic to itself and to Ni-based superalloy. *International Journal of Refractory Metals and Hard Materials*, *18*(1), 33-37.

Liu, Lin & Zhang, Jun & Ai, Cheng. (2020). Nickel-Based Superalloys. 10.1016/B978-0-12-803581-8.12093-4.

Long, F., Yoo, Y. S., Jo, C. Y., Seo, S. M., Jeong, H. W., Song, Y. S., ... & Hu, Z. Q. (2009). Phase transformation of η and σ phases in an experimental nickel-based superalloy. *Journal of alloys and compounds*, *478*(1-2), 181-187.

Minasyan, T.; Aydinyan, S.; Toyserkani, E.; Hussainova, I. In Situ $Mo(Si,Al)_2$-Based Composite through Selective Laser Melting of a $MoSi_2$-30 wt.% AlSi10Mg Mixture. Materials 2020, 13, 3720. https://doi.org/10.3390/ma13173720

Mohammadkhani, S., Jajarmi, E., Nasiri, H., Vahdati-Khaki, J., & Haddad-Sabzevar, M. (2016). Applying FeAl coating on the low carbon steel substrate through self-propagation high temperature synthesis (SHS) process. *Surface and Coatings Technology*, *286*, 383-387.

Mossino, P. J. C. I. (2004). Some aspects in self-propagating high-temperature synthesis. *Ceramics International*, *30*(3), 311-332.

Mouritz, A. (2012). *Introduction to Aerospace Materials: Superalloys for gas turbine engines.* (pp. 251-267) doi:10.1533/9780857095152.251

Munir, Z. A., & Anselmi-Tamburini, U. (1989). Self-propagating exothermic reactions: the synthesis of high-temperature materials by combustion. *Materials Science Reports*, *3*(7-8), 277-365.

Pusavec, F., Deshpande, A., Yang, S., M'Saoubi, R., Kopac, J., Dillon Jr, O. W., & Jawahir, I. S. (2014). Sustainable machining of high temperature Nickel alloy–

Inconel 718: part 1–predictive performance models. Journal of Cleaner Production, 81, 255-269.

Rao, K. A. (2018). Nickel Based Superalloys–Properties and Their Applications. *International Journal of Management, Technology And Engineering*, *8*, 268-277

Reed, R. C., & Rae, C. M. F. (2014). Physical metallurgy of the nickel-based superalloys. In *Physical metallurgy* (pp. 2215-2290). Elsevier.

Shchukin, A. S., & Sytschev, A. E. (2019). Peculiarities of a NiAl/Mo transition zone formed during self-propagating high-temperature synthesis. *Physics of Metals and Metallography*, *120*, 848-852.

Shekari, M., Adeli, M., Khobzi, A., Kobashi, M., & Kanetake, N. (2017). Induction-activated self-propagating, high-temperature synthesis of nickel aluminide. *Advanced Powder Technology*, *28*(11), 2974-2979.

Subrahmanyam, J., & Vijayakumar, M. (1992). Self-propagating high-temperature synthesis. Journal of MaterialsScience, 27,6249-6273. DOI:10.1007/BF00576271

Subrahmanyam, J., & Vijayakumar, M. (1992). Self-propagating high-temperature synthesis. Journal of MaterialsScience, 27,6249-6273. DOI:10.1007/BF00576271

Sytschev, A. E., Vrel, D., Boyarchenko, O. D., Vadchenko, S. G., & Sachkova, N. V. (2013). Load-assisted SHS joining of NiAl to Ni. *International Journal of Self-Propagating High-Temperature Synthesis*, *22*, 52-55.